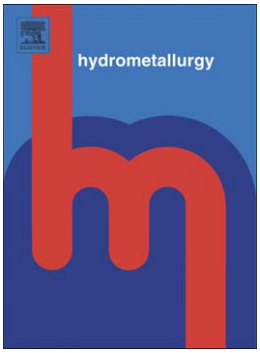

A review of chloride assisted copper sulfide leaching by oxygenated sulfuric acid and mechanistic considerations

G. Senanayake

PII: S0304-386X(09)00050-4
DOI: doi: 10.1016/j.hydromet.2009.02.010
Reference: HYDROM 2961

To appear in: *Hydrometallurgy*

Received date: 27 June 2008
Revised date: 19 February 2009
Accepted date: 20 February 2009

Please cite this article as: Senanayake, G., A review of chloride assisted copper sulfide leaching by oxygenated sulfuric acid and mechanistic considerations, *Hydrometallurgy* (2009), doi: 10.1016/j.hydromet.2009.02.010

A review of chloride assisted copper sulfide leaching by oxygenated sulfuric acid and mechanistic considerations

G. Senanayake*

Parker Centre, Faculty of Minerals and Energy, Murdoch University, Perth, WA 6150, Australia

Abstract

The beneficial effect of chloride on sulfide leaching in sulfuric acid has been widely reported over the last 3 to 4 decades but the reasons have not been resolved. A review of recent literature shows that sulfide leaching is complex due to alternative reaction paths, competitive reactions and interim compounds formed on solid surfaces or in solutions. This study focuses on analysis of rate data for covellite leaching by oxygenated sulfuric acid in the presence of sodium chloride and comparison with the leaching data of chalcocite. The published results for initial copper leaching from covellite are analysed on the basis of a shrinking particle kinetic model to determine the apparent rate constants and reaction orders with respect to the concentrations of chloride, dissolved oxygen, and hydrogen ions. The first stage leaching of chalcocite to an intermediate CuS appears to be controlled by the mass transport of oxygen to the sulfide surface. A comparison has been made between the second stage leaching of chalcocite and the initial leaching of pure covellite to produce elemental sulfur by considering the effect of temperature on dissolved oxygen concentration and apparent rate constants. The Arrhenius plots gave comparable values for activation energy for covellite (101 kJ. mol^{-1}) and second stage leaching of chalcocite (96 kJ mol^{-1}). A linear correlation of stability constants was used to determine equilibrium constants for the formation of CuS_2 and Cu(OH)(Cl). The peak potentials of voltammograms of covellite are in reasonable agreement with the predicted potentials based on thermodynamics of a range of solid phases including CuS, CuS_2, Cu(OH)Cl, and $Cu_2Cl(OH)_3$. These observations are used to propose a reaction mechanism via mixed-ligand complex species.

Keywords: Covellite; Chalcocite; Sulfuric acid-oxygen leaching; Chloride effect; Kinetics; Mechanism.

*tel.: +61 8 93602833; fax: +61 8 93606343. Email: G.Senanayake@murdoch.edu.au

1. Introduction

The thermodynamic and kinetic basis for the rationalisation of the beneficial effect of chloride ions on sulfide leaching in non-sulfate systems such as strong brines has been widely reported (Peters, 1977; Winannd, 1991; Majima, 1995; Dutrizac, 1992; Muir, 2002; Flett, 2002; Senanayake and Muir, 1988, 2003). The HydroCopper^{TM} process uses copper(II) chloride in strong brine (4.3 mol.dm^{-3} NaCl) to leach chalcopyrite concentrates at pH 1.5-2.5 and near boiling point of water (Lundstrom et al., 2005). New process flowsheets have been developed for chalcopyrite concentrates which include leaching in acidic calcium chloride solutions (~2 mol.dm^{-3} Cl^-) followed by conventional solvent extraction, stripping as sulfate, electrowinning, and iron removal as goethite or hematite (Liddicoat and Dreisinger, 2007).

The beneficial effect of low chloride addition for the leaching of copper-nickel sulfides in sulfate systems, previously reported by Subramanian and Ferrajuolo (1976), has also attracted renewed interest in atmospheric and pressure oxidation processes for a range of sulfides (Lu et al., 2000a,b; Deng et al., 2001; Berezowsky and Trytten, 2002; Peacy et al., 2003; Ferron et al., 2003; Kinnunen and Puhakka, 2004; McDonald and Muir, 2007a,b; Carneiro and Leao, 2007). For example, low chloride has a beneficial effect upon the acid-pressure leaching of copper and nickel from finely ground sulfide concentrates in the ACTIVOX process (Johnson and Streltsova, 1999). Low chloride also shows a beneficial role in PLASTOL, BHAS, CESL, and bioleaching processes (Ferron et al., 2003; Peacey et al., 2003; Defreyne et al., 2006; Watling, 2006).

Despite some detailed studies, reasons for the beneficial role of low chloride in sulfide leaching in sulfate systems remain unresolved (Cheng and Lawson, 1991a,b; Fisher et al., 1992; Kinnunen and Puhakka, 2004; Brown and Papangelakis, 2005; Carneiro and Leao, 2007). The general view is that during atmospheric leaching in the presence of sodium chloride in sulfuric acid, a porous and somewhat crystalline sulfur layer is formed on the sulfide surface, instead of a tight passivating sulfur layer which blocks the surface (Cheng and Lawson, 1991a, Muir and Ho, 2006; Carneiro and Leao, 2007). Elemental sulfur formed during the leaching of chalcopyrite with ferric chloride is also more porous than that formed with ferric sulfate, thus the leaching rate is an order of magnitude larger in the former (Majima et al., 1985).

Peters (1976a) reported that chalcopyrite, the primary and most important sulfide mineral of copper, is most difficult of the copper sulfides for hydrometallurgical treatment due to slow leaching kinetics. Recent reviews have highlighted the growing interest and conflicting views amongst researchers to understand the mechanistic details of leaching of chalcopyrite and secondary copper minerals in order to promote hydrometallurgical routes to extract copper (Dreisinger, 2006; Watling, 2006; Nicol, 2007; Klauber, 2008; Cordoba et al., 2008a). Chalcocite and covellite are two of the common copper-bearing minerals also formed as intermediate products during the leaching of chalcopyrite, copper matte/residue and copper-nickel sulfides; as shown by some of the reactions relevant to the present study listed in Table 1 (Peters, 1976a,b; Grizo et al., 1982; McDonalds and Langer, 1983; Cheng and Lawson, 1991a,b; Fisher et al., 1992; Grewal et al., 1992; Rademan et al., 1999; Muir and Ho, 2006; Deng et al., 2001; Provis et al., 2003; Nicol and Lazaro, 2003; Ruiz et al., 1998, 2007; Dreisinger, 2006; Herreros et al., 2006; Herreros and Vinals, 2007, Cordoba et al., 2008a,b). The dissolution of nickel sulfides via the displacement reactions such as reactions R6-R8 in

Table 1 (Rademan et al., 1999; Muir and Ho, 2006) is thermodynamically more favourable with large values of equilibrium constants, compared to the acid dissolution via reactions R4-R5. Moreover, the copper sulfide formed on the surface of millerite via reaction R6 is oxidized more rapidly than the base mineral (Miki and Nicol, 2008a). The oxidative dissolution of covellite by oxygen according to reaction R14 is also thermodynamically more favourable ($K_{298\ K} = 10^{20}$), compared to non-oxidative acid dissolution according to reaction R9 ($K_{298\ K} = 10^{-16}$). However, a range of stable or interim products can be predicted from the published thermodynamic data as noted in reactions R10-R18, all with favourable equilibrium constants. For example, the beneficial effect of chloride ions on the oxygenated-acid dissolution of copper from synthetic Cu_2S particles (Cheng and Lawson, 1991a) and acid dissolution of copper from synthetic CuO discs (Majima et al., 1980) has been rationalised by considering the formation of an interim adsorbed complex species of the formula: $Cu(OH)(Cl)^0$ (Senanayake, 2007b,c; 2008b).

The objectives of this investigation are: (i) to briefly review the complexity of leaching of copper sulfide ores/concentrates and mechanistic considerations, with special attention to the formation of interim compounds and competitive reactions in solid state or solution; (ii) to present a quantitative analysis of published data for the dissolution of similar sized covellite particles in the presence of sodium chloride (Cheng and Lawson, 1991b); and (iii) to highlight the importance of considering a surface reaction which involves mixed-ligand complexes of copper(II) with chloride and hydroxide ions. The aim is to rationalise the leaching behaviour of complex or mixed sulfides and the selection of conditions for accelerated leaching to produce sulfur and iron oxide products.

2. Complexity of mechanistic studies

Results based on the dissolution of sulphide particles in batch leaching experiments can be successfully used to investigate the rate controlling steps and mechanistic details of leaching of metals/minerals, especially if a comparison can be made between the rates based on flat surfaces and particles (Parker et al., 1981). However, a quantitative analysis of leaching kinetics of complex/mixed sulfides and nickel-copper mattes presents a number of challenges due to the complexity of the dissolution mechanism caused by a range of competing factors depending on mineralogy:

(i) alternative pathways of non-oxidative and/or oxidative leaching behaviour of different sulfides in acid media,

(ii) possible involvement of more than one redox couple as oxidants, such as Fe(III)/Fe(II), Cu(II)/Cu(I), O_2/H_2O, O_2/H_2O_2, and H_2O_2/H_2O,

(iii) formation of elemental sulfur, thiosulfate, sulfite, and sulfate as the interim/final oxidation product(s) of sulfide depending on the conditions,

(iv) difficulty in detection/characterisation of some solution/surface species or interim solid metal-sulfur phases,

(v) galvanic interactions caused by host minerals,

(vi) passivation or blockage of mineral surface by insoluble products,

(vii) beneficial or detrimental effects caused by background reagents.

Thus, the rate analysis based on individual sulfides allows a better understanding of the mechanism of surface reactions corresponding to dissolution, passivation, and de-passivation. Some examples follow.

Hirato et al. (1989) conducted a comparative study of chemical and electrochemical dissolution of copper from sintered CuS discs in acidified iron(III) chloride solutions.

The half order reaction with respect to Fe(III) concentration supported an electrochemical mechanism for the dissolution. Nicol (2007) noted the importance of considering the formation of sulfur during leaching via two different mechanisms for a range of base metal sulfides. Firstly, direct oxidation by an oxidant such as Fe(III) leads to the precipitation of sulfur on the mineral surface which may block the surface. Secondly, non-oxidative acid dissolution of sulfide and indirect oxidation of hydrogen sulfide by Fe(III) in solution leads to the precipitation of sulfur in the bulk. The rate of dissolution of a sulfide mineral MS under acidic conditions can be estimated by considering the equilibrium constants for the dissolution of MS to M(II) and H_2S. Here, the rate controlling step is the rate of mass transfer of products such as M(II) and H_2S away from surface, shifting the dissolution equilibrium in the forward direction with time (Nicol and Lazaro, 2003; Nicol, 2007).

3. Effect of chloride on redox potentials and leach results

The possibility of involvement of more than one redox couple as oxidant(s) is evident from Fig. 1a. where the potentials in oxygenated chloride systems follow the descending order O_2/H_2O > Fe(III)/Fe(II) > Cu(II)/Cu(I). It is widely accepted that in such systems with chloro-complexes the redox couples Cu(II)/Cu(I) (fast) or Fe(III)/Fe(II) (slow) can oxidize the sulfide mineral or hydrogen sulfide, whilst the oxidation of Cu(I) to Cu(II) by Fe(III) or dissolved oxygen reproduces the oxidant for leaching (Parker et al., 1981; Nicol and Lazaro, 2003; Nicol, 2007; Miki and Nicol, 2008a). Lee et al. (2008) showed that in chloride medium the cathodic current for the reduction of Cu(II) on a covellite surface is larger than that for the reduction of dissolved oxygen, which results in faster dissolution of covellite in the presence of

copper(II). The rapid equilibration Cu(II) + Fe(II) = Cu(I) + Fe(III) and the rapid oxidation of Cu(I) to Cu(II) by dissolved oxygen rationalises the catalytic effect of Cu(II) on the oxidation of Fe(II) (Miki and Nicol, 2008b).

The leaching of chalcocite/covellite by oxygen represented by the potential-pH diagram in Fig. 1b shows the oxidation of Cu_2S via CuS to produce elemental sulfur and $CuCl^+$, $Cu_2Cl(OH)_3$, or $Cu(OH)_2$/CuO depending on pH at 25 - 90^oC. Fig. 1b does not show the thermodynamically unstable copper(I) species. It also does not consider the species such as $Cu(OH)_2^-$ and $Cu(OH)_n^{-(n-2)}$ (n = 1-4) which are formed in solutions of high pH in the absence of other complexing media (Beverskog and Puidomenech (1997). Nevertheless, the rapid oxidation of Cu(I) by dissolved oxygen produces $CuCl^+$ which is converted to $Cu(SO_4)^0$ in a predominantly sulfate system. Thus, the rationalisation of initial leaching of synthetic covellite by oxygen in iron-copper-free sulfate solutions would be less challenging than that of complex/mixed sulfides and would produce more comprehensive information on the role of chloride ions during the oxidation of covellite by oxygen in a sulfate background.

Fig.2a shows the results of atmospheric leaching of copper from synthetic covellite by oxygen after 1 or 6 h (Cheng and Lawson, 1991b). The beneficial effect of chloride addition increases up to a concentration of 0.5 mol.dm^{-3} NaCl where the copper extraction exceeds 80% after 6 h. According to Fig.2b, the copper leaching from synthetic chalcocite by oxygen is faster than that from covellite and reaches about 70% after 20 min (Cheng and Lawson, 1991a). The reaction order with respect to oxygen pressure was found to be 0.3 in the case of covellite in the presence of sodium chloride (Cheng and Lawson, 1991b). Although no physical significance for this order was given, the chloride ions were considered to promote the porosity of the sulfur layer formed on the covellite surface. However, the rationalisation of kinetics of chalcopyrite

poses more challenges with regard to the different reaction pathways that may produce different product layers responsible for slow leaching. Further studies are essential to compare, contrast, rationalise, and quantify the beneficial effect of chloride ions at a low concentration in a sulfate system.

4. Interim copper compounds

An understanding of the nature of interim compounds and competitive reactions at the surface of sulfide minerals or in solution plays an important role in successful elucidation of reaction mechanisms. Different types of interim compounds in the solid state have been considered in the mechanistic interpretation of copper sulfide leaching. They are sulfides, oxides, and chlorides or mixed chloro-hydroxides. In addition, copper(I) chlorides and a number of interim sulfur species in solution have also been reported.

4.1 Copper sulfide reactions

According to the potential-pH diagram of Cu-Fe-S-O-H_2O system the acid dissolution of $CuFeS_2$ takes place via intermediate sulfides such as Cu_5FeS_4, CuS, and Cu_2S (Peters, 1976b; Cordoba et al., 2008a). The reaction mechanisms of dissolution/passivation of secondary copper sulfides are relatively simple compared to that of chalcopyrite, but involves a number of interim species. Despite the ionic formula of Cu_2S_2 reported in the literature, it has been general practice, for simplicity, to use the formula CuS in chemical reactions to represent covellite (Fisher et al.,1992; Goh et al., 1996). Koch and McIntyre (1976) identified four intermediate phases: $Cu_{1.95\text{-}1.91}S$,

$Cu_{1.86-1.80}S$, $Cu_{1.68-1.65}S$, and $Cu_{1.40-1.36}S$ formed during electrochemical oxidation of covellite. These phases have been characterised by XRD and in-situ treatment of reflectance spectra. The oxidative dissolution of chalcocite by Fe(III), Cu(II), or oxygen is a multistage process which involves the initial fast oxidation via djurleite ($Cu_{1.93}S$) and digenite ($Cu_{1.8}S$) to blue-remaining covellite ($Cu_{1.0-1.2}S$): followed by the slow oxidation of $Cu_{1.0-1.2}S$ (Sullivan, 1933; Mao and Peters, 1983; McDonald and Langer, 1983; Rademan et al., 1999, Cheng and Lawson, 1991a,b; Fisher et al., 1992). The non-oxidative acid decomposition of chalcopyrite produces chalcocite and covellite (Peters, 1976a,b), while the chemical metatheses of chalcopyrite in the presence of Cu(II) ions produces covellite and digenite (Sequeira et al., 2008).

Gerlach and Kuzeci (1983) conducted an electrochemical study of covellite and the results were rationalised on the basis of the formation of non-stoichiometric compounds, solid state diffusion of copper ions, and chemical dissolution. Bertram and Hillrichs (1981), and Hillrichs and Bertram (1983a,b) interpreted current-voltage curves for the anodic dissolution of synthetic/natural chalcocite and covellite discs in sulfuric acid solutions on the basis of the formation of metastable non-stoichiometric copper oxide or hydroxides. Based on cyclic voltammograms of CuS in sulfuric acid medium, Hillrichs and Bertram (1983a) considered the formation of intermediate oxides: $CuS \rightarrow CuO_{0.67(brown)} \rightarrow CuO_{(black)}$. Although the formation of these oxides stopped the total anodic decomposition of CuS, subsequent decomposition was evident from hindrance of Cu^{2+} flux by adherent sulfur on the anode surface at higher potentials. The addition of surface active anions such as Cl^-, ClO_4^-, and NO_3^- caused a further activation of CuS, indicating the importance of considering the role of anions. Miki and Nicol (2008a) reported linear sweep voltammograms of synthetic covellite in a mixed H_2SO_4/NaCl system which showed that the active dissolution at low potentials was followed by

passivation at about 0.6 V (SHE), whilst the anodic currents increased as the chloride concentration was increased from 0.2 mol.dm^{-3} to 2 mol.dm^{-3}. The potential-pH diagram in Fig. 1b predicts the dissolution of CuS to form $CuCl^+$ as well as the passivation due to the formation of insoluble S or $Cu_2Cl(OH)_3$ at a potential close to 0.6 V at 25^{o}C and 90^{o}C.

4.2 Interim chlorides and mixed chloro-hydroxides

Fisher et al. (1992) considered the formation of copper(I) chloride and sulfate ions in the anodic half reaction of covellite. In oxygenated chloride solutions, the rate of copper extraction from a chalcocite concentrate (at 70 ^{o}C) was seventy times faster than that in oxygenated sulfate systems. This was related to the formation of $CuCl_3^{2-}$ in the anodic reaction for dissolution at both stages (Cu_2S and CuS). It was noted that dissolved oxygen was reduced to water via hydrogen peroxide but sulfide was converted to sulfate in the second stage (Fisher et al., 1992). However, equations R34 and R35 in Table 2 represent the reaction steps and widely reported anodic and cathodic half cell reactions. These reactions lead to the formation of Cu(II) ions and elemental sulfur as major products according to the thermodynamically favourable overall reaction R14 in Table 1.

Cheng and Lawson (1991b) noted that the formation of copper(I) chlorides such as $CuCl_2^-$ in sulfuric acid media in the presence of sodium chloride is only possible at higher pulp densities, where there is inadequate mass transfer into the liquid phase, causing oxygen deficiency during leaching. Nicol (2007) proposed that the formation of Cu(I) and elemental sulfur in oxygenated chloride solutions is a result of the reaction between Cu(II) and hydrogen sulfide. Peters (1976b), McDonald and Langer (1983),

Cheng and Lawson (1991a), and Muir (2002) reported the formation of basic copper chloride $Cu_2(OH)_3Cl$, i.e. $Cu(OH)(Cl).Cu(OH)_2$. A potential-pH diagram which shows the predominant areas of $CuCl^+$ and Cu(OH)Cl species in solutions of pH < 7 was published by Sabba and Akretche (2006). The precipitation of $Cu_2(OH)_3Cl$ has been observed at pH 4 in leaching experiments with covellite conducted with small monosized particles (13 μm) at low initial sulfuric acid concentrations of 5.10^{-3} $mol.dm^{-3}$. The copper extraction increased in the first three hours, but then decreased as a result of an increase in pH to 4. Thus, Cheng and Lawson (1991b) proposed the overall reaction which involved the formation of $CuCl^+$ (R15) in acid solutions at low pH.

5. Competitive reactions and sulfur products

Base metal sulfide minerals are likely to undergo oxidation with oxygen by two different reaction pathways via elemental sulfur or thiosulfate depending on the conditions such as ammoniacal leaching, or acid leaching at atmospheric or elevated pressures (Muir et al., 1981; McDonald and Muir, 2007a). Rotating ring-disc electrochemical studies with nickel matte (Ho, 1996) and chalcopyrite (Lazaro and Nicol, 2006) have revealed the formation of interim sulfur-oxy species such as thiosulfate. Under some leaching conditions, NiS_2 and FeS_2 produce sulfate ions rather than elemental sulfur, while chloride ions appear to modify the passivating sulfur or inhibit the formation of NiS_2 layers (Muir and Ho, 2006).

Quantitative analysis of sulfur products of covellite oxidation by oxygen in mixed systems such as H_2SO_4-NaCl with a low concentration of NaCl revealed that the majority of sulfide was oxidized to elemental sulfur by oxygen (Cheng and Lawson, 1991b). A reaction scheme based on the formation of intermediates $H_2S_2O_2$ and

H_2SO_3 has been proposed to account for the quantitative yields of sulfate ions and elemental sulfur during sulfide leaching (Lotens and Wesker, 1987). The oxidation products of sulfides would depend upon whether: a "one-electron transfer" takes place by oxidants such as Cu(II) or Fe(III), or a "two-electron transfer" takes place by oxidants such as chlorine or hydrogen peroxide at the solid/liquid interface. In the former case the reaction via $2H_2S_2O_2 = 3S + H_2SO_3 + H_2O$ would yield 75% elemental sulfur whilst the reaction $2H_2SO_2 = S + H_2SO_3 + H_2O$ would yield 50% elemental sulfur. Moreover, the increase in yield of elemental sulfur in acidic solutions of low pH is a result of the formation of H_2S due to acid dissolution of a metal sulfide, followed by the reaction $H_2S + H_2S_2O_2 = 3S + 2H_2O$ (Lotens and Wesker, 1987). Thus, sulfate formation has been ignored in the kinetic analysis of sulfide oxidation. Nevertheless, the final copper(II) product of chalcocite /covellite oxidation in oxygenated sulfuric acid solutions with low sodium chloride is the thermodynamically stable ion-pair $Cu(SO_4)^0$ shown in reaction R16 (Table 1).

Miki and Nicol (2008a) reported the similarities of voltammetric peak potentials and the potentiometric current transients of covellite and chalcopyrite. The onset of the transpassive region during chalcopyrite oxidation has been considered as an indication of the formation of covellite (Viramontes-Gamboa et al., 2007). The leaching results have also demonstrated that chalcopyrite dissolves through the formation of covellite and subsequent oxidation of covellite in iron(III) sulfate solutions (Cordoba et al., 2008b). These facts support the dissolution mechanism of chalcopyrite via reaction R1 in Table 1 proposed by Peters (1976b) and Nicol (2007) and justify the extension of the present discussion on the basis of electrochemical active-passive behaviour of covellite to discuss reasons for passivation in sulfate media, and non-passivating role of chloride in sulfate systems.

Muir and Ho (2006) described the beneficial effect of chloride in nickel sulfide leaching as a result of inhibition of the formation of a passivating layer of NiS_2. By analogy with reactions of NiS, it would seem that passivation of CuS due to formation of CuS_2 is inhibited by chloride via an electrochemical mechanism (Muir, 2009). The Raman spectroscopic studies by Parker et al. (2003) also provide some evidence for the disruption of the formation of disulfide type layer on chalcopyrite surface in the presence of chloride. However, subsequent studies by Parker et al. (2008a-b) using surface enhanced Raman scattering of chalcopyrite surface showed similar oxidation products in both hydrochloric and sulfuric acid solutions. The surface species with S-S bonding in transpassive region were not characteristic of polysulfide or polythionates. The production of oxidation products with S-S bonds at lower potentials in sulfuric acid, than that in hydrochloric acid, appeared to be a result of the mechanistic or ionic strength differences in the sulfate and chloride systems (Parker 2008b).

Based on electrochemical and XPS studies, the dissolution/passivation products formed during electrochemical oxidation of chalcopyrite in 1 mol dm^{-3} perchloric acid were identified as Fe^{2+} and metastable CuS_2^* at lower potentials (~0.74 V) and elemental sulfur at higher potentials (> 1.24 V) (Yin et al., 1995). Buckley and Woods (1984) considered the depletion of iron and conversion of chalcopyrite to (i) CuS_2 after exposure to air for several weeks, or (ii) $Cu_{0.8}S_2$ after conditioning in acid solutions. The structure of the metastable phase CuS_2^* formed on the surface (passive film) has not been identified, but reported to be different from that of pyrite. A wide variety of experimental techniques have shown that CuS_2 has a monovalent (d^{10}) rather than a divalent (d^9) oxidation state of copper (Ueda et al., 2002). If the chalcopyrite structure is represented by an ionic bonding model $(Cu^+)(Fe^{3+})(S^{2-})_2$ (Crundwell, 1988; Mikhlin et al., 2004), the formation of a passive film according to the anodic reaction

$(Cu^{+})(Fe^{3+})(S^{2-})_2 = CuS_2 + Fe^{2+} + 2e^{-}$ can be considered with a possible change in oxidation states $(Cu^{+})(S_2^{-})$ proposed by Yin et al. (1995). Another possibility is the redox or precipitation reaction to produce CuS_2 on the surface, from ions in solution: $Cu^{2+} + S_2^{2-} = (Cu^{+})(S_2^{-})$, where the disulfide (S_2^{2-}) can be formed by the oxidation of H_2S formed by non-oxidative dissolution (reaction R40 in Table 2).

Hackl et al. (1995) described chalcopyrite dissolution as a two stage reaction: (i) formation of intermediate disulfide $Cu_{1-x}Fe_{1-y}S_2$ ($y>>x$ and $x+y \sim 1$) during pressure oxidation due to preferential initial leaching of iron, and (ii) slow dissolution of copper from the disulfide producing a copper polysulfide ($Cu_{1-x-z}S_2$) causing passivation. Klauber et al. (2001) ruled out the formation of polysulfide CuS_n ($n>2$) and noted the possibility of formation of only a few atomic layers of the non-stoichiometric $Cu_{0.8}S_2$. Thus, it is important to estimate the formation constants of CuS_2 to improve the understanding of passivation reaction(s) of copper sulfides.

6. Formation constants of interim copper species

6.1 CuS_2 Species

Table 3 lists equilibrium constants for the formation of various ionic or neutral complex species and insoluble salts of Cu(II) and Fe(II) for comparison. The approximate linear correlation of formation constants of Cu(II) and Fe(II) complexes in Fig. 3b can be used to predict the formation constants at 25°C: $Cu(HS)_2^0$ ($\sim 10^8$), CuS_2 ($\sim 10^{39}$). The values shown in brackets were calculated by substituting the reported values for $Fe(HS)_2$ ($10^{2.2}$) and FeS_2 (10^{26}) from Young et al. (2003) and HSC 6.1 data base in the mathematical expression representing an approximately linear correlation in

Fig. 3a. This allows the calculation of approximate values of standard reduction potentials for reactions involving CuS_2 listed in Table 2 (R43, R46, R47). The lower values of E^o for the corresponding nickel couples listed in Table 2 indicates the passivation of NiS by NiS_2 at a lower potential. A potential-pH diagram for Ni-S-H_2O system that shows a large stability region of NiS_2 in the potential range 0-0.25 V in acidic media was published by Muir and Ho (2006).

Cyclic voltammetric investigations of the dissolution of covellite in 1 mol dm^{-3} H_2SO_4 at 20^{o}C have shown that the decomposition of CuS starts at 0.56 V (Hillrichs and Bertram, 1983). This is consistent with E^o = 0.53 V for reaction R46 in Table 2. The peak potential of 0.72 V of the cyclic voltammogram of CuS in sulfuric acid media is also in excellent agreement with the calculated E^o = 0.72 V for reaction R43. However, visual evidence for sulfur formation was found after anodization at a much higher potential of 2.35 V (Hillrichs and Bertram,1983). In contrast, the current-potential curve of NiS in 0.5 mol dm^{-3} H_2SO_4 showed a peak at a lower potential of ~1.34 V (Muir and Ho, 2006). Moreover, anodic oxidation of NiS produced S, NiS_2 and $S_2O_3^{2-}$ at a potential of ~1 V in mixed sulfate/chloride media. These differences warrant further electrochemical studies and discussion beyond the scope of the present study. Here, the main focus is the beneficial role and the de-passivation effect of chloride ions during oxidation of covellite by oxygen.

6.2 Cu(OH)(Cl) species

If oxygen is adsorbed on the surface, as noted by Fisher et al. (1992), the direct oxidation represented by reaction R14 will produce sulfur on the sulfide mineral surface. Other reactions in Table 1 represent the non-oxidative or oxidative dissolution

of covellite and the proposed role of the common anion X^-. For example, the formation of ion-pairs HSO_4^- and $Cu(SO_4)^0$ is taken into account in reactions R10 and R16, while the formation and reaction of interim mixed complexes Cu(SH)(X) and Cu(OH)(X) is considered in reactions R21-R27. McDonald and Langer (1983) considered the formation of $Cu(OH)(Cl)_x^{(1-x)}$ during the leaching of copper sulfides and estimated the formation constants $10^{10.5}$ (25°C) and $10^{9.1}$ (105°C). Fig. 3a shows a linear correlation of the logarithmic values of equilibrium constants listed in Table 3 for Cu(II) and Pb(II). An equilibrium constant of $10^{13.7}$ has been reported for the formation of $Pb(OH)(Cl)_s$ (Wagman et al., 1982). This value can be used in the equation for the linear correlation in Fig. 3a to predict the relevant equilibrium constant of $10^{14.2}$ for the formation of $Cu(OH)(Cl)_s$ at 25°C. The calculated concentration of Cu^{2+} in 0.5 mol dm^{-3} NaCl solution at pH 4 is $9.5.10^{-4}$ mol.dm^{-3}. This explains the precipitation of copper at low acidities as observed by Cheng and Lawson (1991a).

It can be seen from Table 3 and Fig. 3a that the magnitudes of formation constants of complex species or solids from Cu^{2+} ions are comparable to those from Pb^{2+} ions. This may be related to the comparable softness of Cu^{2+} and Pb^{2+} (Fig. 4). Softness is a property related to the polarizability of ions (Marcus, 1997). According to the concept of soft and hard acids and bases (Pearson, 1973), soft ions prefer forming complexes with soft ligands. It is reasonable to suggest, on the basis of the apparent descending order of softness $S^{2-} > HS^- > OH^- > Cl^-$ in Fig. 4, that the thermodynamically favourable oxidative dissolution process of CuS to $Cu(SO_4)^0$ by oxygen in acidic sulfate media would involve the three step transformation:

$$CuS \rightarrow Cu(SH)(Cl) \rightarrow Cu(OH)(Cl) / S \rightarrow Cu(SO_4)^0 / S$$

(i) (ii) (iii)

as described in reactions R24, R25, R26, and R29, as a result of (i) protonation and adsorption of Cl^-, (ii) reaction with O_2, and (iii) reaction with HSO_4^-, .

A comparison of rate data for the dissolution of covellite in the absence or presence of chloride ions also supports the formation of Cu(OH)(Cl) as an interim species. A low rate was observed for chloride-free leaching of covellite in 0.5 mol dm^{-3} HNO_3 and 0.25 mol dm^{-3} H_2SO_4 solutions at 90 ^oC under an oxygen pressure of 101.3 kPa, where < 10% copper was leached after 6 h. However, the leaching was enhanced by the addition 0.5 mol.dm^{-3} NaCl to both acids. Leaching at 101.3 kPa oxygen pressure in the two cases: (i) 0.5 mol.dm^{-3} HNO_3 + 0.5 mol.dm^{-3} NaCl, and (ii) 0.25 mol.dm^{-3} H_2SO_4 + 0.5 mol.dm^{-3} NaCl showed identical leaching curves and > 80% copper extraction after 6 h (Cheng and Lawson, 1991b). These results were also identical to those obtained with 0.5 mol dm^{-3} HCl, indicating that the beneficial role of chloride ions is due to the involvement of the anion X^- as in reactions R21-R23, and the stronger complexation when $X^- = Cl^-$, compared to $X^- = HSO_4^-$. Further support for the beneficial role of chloride ions in the surface reaction is evident from rate analyses based on heterogeneous kinetic models described in section 7.

7. Rate data and kinetic models for covellite

Cheng and Lawson (1991b) reported the effect of temperature (75-95^oC), oxygen partial pressure (5.1-101.3 kPa), particle size (13-56 μm), and concentration of sulfuric acid (0.005 – 2 mol.dm^{-3}) and sodium chloride (0.01-2 mol.dm^{-3}) on the leaching of mono-sized covellite particles at a solid/liquid ratio of 1 g dm^{-3}, and an agitation speed of 1000 rpm in batch leaching. The rate data for dissolution during first two hours obeyed a non-porous shrinking particle (sphere) kinetic model described by Eq. 1.

$$1-(1-X_B)^{1/3}=\left(\frac{bk_BC_A}{r_o\rho}\right)t=k_{ss}t \qquad (1)$$

This model considers: (i) a surface reaction of a solid B with a reactant A of concentration C_A (mol.m^{-3}) in solution at a stoichiometric molar ratio of B/A = b/1, A(aq) + bB(s) → products, and (ii) a decrease in surface area due to the decrease in initial particle radius r_o (m) with time t (s) (Levenspiel, 1972). The terms ρ (mol m^{-3}) and k_{ss} (s^{-1}) represent the molar concentration of reacting metal in solid B and the apparent rate constant, respectively, while X represents the fraction of metal leached after time t. The term k (m s^{-1}) in Eq. 1 represents the intrinsic rate constant of the surface reaction, which has the same units as the mass transfer coefficient.

Fig. 5 shows the applicability of Eq. 1 for the dissolution of covellite during initial leaching over 2 h at different oxygen partial pressures. Similar plots were used to determine the apparent rate constants listed in Table 4 from the slopes of linear relations, such as in Fig. 5. The increase in rate constant with increase in temperature from 75 ^{o}C to 95^{o}C obeyed the Arrhenius equation $k = A\, e^{(-E/RT)}$ with an activation energy of E = 77 kJ.mol^{-1} (Cheng and Lawson, 1991b). According to Eq. 1, a decrease in particle size from 58 μm to 28 μm is expected to increase the value of k_{ss} by a factor of 58/28 = 2.1/1. This is consistent with the observed ratio 2/0.9 = 2.2/1 of k_{ss} values of tests G1 and G2 in Table 4. Thus, all the results indicate surface reaction controlled dissolution kinetics of covellite over the initial period of one or two hours.

Other forms of Eq. 1 have also been employed by researchers - depending on the minerals and reagents that affected the surface reaction. For example, copper leaching from chalcopyrite particles by oxygenated acid solutions has been rationalised on the basis of Eq.2. In such cases empirical values of K, b_Bk_B have been useful in predicting leaching performance under different conditions (Lin and Sohn, 1987). The half order

reaction with respect to H^+ and O_2 shows the electrochemical nature of the surface reaction. Similar analysis of apparent rate constants of covellite leaching is essential for the comparison of measured leaching rates with mass transport calculations.

$$1-(1-X_B)^{1/3} = b_B k_B [H^+]^{0.5} \left(\frac{[O_2]}{1+K[O_2]} \right)^{0.5} t \qquad (2)$$

8. Factors affecting apparent rate constants

A proper analysis of k_{ss} values for covellite leaching as a function of different variables can be complicated due to a number of reasons. Firstly, the change in hydrogen ion concentration in bulk according to the sulfate/bisulfate equilibrium and the sodium ion concentration has to be taken into account by considering the relevant equilibrium constants at elevated temperatures. Fig. 6 shows the change in actual concentration of hydrogen ions at 90^{o}C with increase in acid concentration, while the concentration of sulfate ions remains negligibly small.

Secondly, the dependence of dissolved oxygen concentration on temperature and background electrolytes has to be considered on the basis of empirical relationships proposed by Tromans (1998). The concentration of dissolved oxygen increases with increasing oxygen mole fraction (Table 4), but decreases with increasing concentration of sodium chloride and sulfuric acid. Fig. 7 shows the effect of temperature on oxygen solubility in water based on the equations proposed by Tromans (1998). The effect of temperature on the intrinsic rate constant for the dissolution of B based on the Arrhenius equation can be combined with Eq. 1 to derive Eq. 3. The superscript a in Eq. 3 represents the reaction order with respect to the concentration of reagent A. Thus,

the activation energy, E (kJ.mol^{-1}), based on Eq. 4 is more reliable and suitable for comparison.

$$1-(1-X_B)^{1/3}=\left(\frac{b(A'e^{-E/RT})k_B(C_A)^a}{r_o\rho}\right)t=k_{ss}t \quad (3)$$

$$\ln\left(\frac{k_{ss}}{(C_A)^a}\right)=\ln\left(\frac{bA'}{r_o\rho}\right)-E\left(\frac{10^3}{RT}\right) \quad (4)$$

Thirdly, the formation of elemental sulfur or other products may block the surface/pores. This would change the kinetic behaviour to that described by a shrinking core model: $1\text{-}3(1\text{-}X)^{2/3} + 2(1\text{-}X) = 6\ CDr_o^{-2}\rho^{-1}t$, where D = diffusion coefficient of reactant or product ($m^2\ s^{-1}$) through a porous solid on the surface. For example, Carneiro and Leao (2007) showed the validity of this model for the leaching of chalcopyrite by ferric sulfate in non-chloride solutions. Bertram and Hillrichs (1981) noted that the adsorption of metastable copper oxides (hydroxides) as well as a product layer of S/CuO (Fig. 1b) on the sulfide surface will hinder the copper ion flux during anodic oxidation. It is expected that the beneficial effect of chloride ion is a result of avoiding such product layers or passivating layers of CuS_2 being formed on the sulfide surface. Thus, it is important to consider the effect of the actual concentration of dissolved oxygen, hydrogen ions, and chloride ions on the apparent rate constants, which would lead to reaction orders and activation energy and shed more light on reaction mechanism.

9. Reaction orders and activation energy of covellite leaching

Fig. 8a shows a logarithmic plot of k_{ss} as a function of the concentration of variables such as hydrogen ions, chloride ions, or dissolved oxygen, when the concentration of acid, salt, or oxygen partial pressure was changed in the case of

covellite leaching. The slopes of the linear relationships confirm a reaction order of ~0.5 and ~1 with respect to the concentration of dissolved oxygen and chloride ions, respectively. The reaction orders with respect to hydrogen and chloride ions are approximately zero at higher concentrations. Although the presence of chloride ions is essential in order to increase the rate of dissolution of covellite by dissolved oxygen in sulfuric acid media at 90^{o}C, concentrations of sodium chloride above 0.5 mol dm^{-3} do not significantly influence the rate. This is consistent with many examples reported in the literature, where an increase in background chloride beyond 5-20 g.dm^{-3} in sulfate systems did not show a significant influence on the leaching kinetics and the final copper extraction (Subramanian and Ferrajuolo, 1976; Lu et al., 2000a,b; Deng et al., 2001; Ferron et al., 2002, Kinnunen and Puhakka, 2004; Carneiro and Leao, 2007; Herreros and Vinals, 2007). The results for the first stage leaching of chalcocite described previously (Cheng and Lawson, 1991a, Senanayake, 2007c, 2008b) are shown in Fig.8b for later comparison in section 10.

Cheng and Lawson (1991a) showed that the second stage leaching of chalcocite also obeys a shrinking sphere kinetic model. Fig. 9 plots $\ln\{k_{ss}/(C_{O2})^{0.5}\}$ as a function of (10^3/RT) according to Eq. 4. The second stage leaching of chalcocite and the first stage (initial) leaching of covellite show good linear relationships with y-intercepts close to 29 and slopes corresponding to activation energies of 96 and 101 kJ.mol^{-1}, respectively. These activation energies are higher than the values of 69 and 77 kJ.mol^{-1} reported by Cheng and Lawson (1991a,b), but they support the two stage leaching mechanism of chalcocite, via covellite, and confirm that covellite leaching is controlled by a surface chemical reaction. Further support for the beneficial role of chloride ions on the surface reaction is evident from the mass transfer calculations described below.

10. Intrinsic rate constant and mass transfer coefficient

Previous researchers showed the importance of comparing experimental intrinsic rate constants or rates per unit surface area with the estimated values based on mass transfer coefficients, in order to examine the chemical or mass transport controlled nature of the surface reaction (McCarthy et al., 1998; Nicol and Lazaro, 2003; Nicol, 2007). Following previous work by Raschman and Fedorockova (2006), the experimental value of k_B in Eq. 1 can be compared with the mass transfer coefficient (k_m) based on Eqs. 5-8 (Cussler, 1997):

$$k_m = \frac{ShD}{L} \tag{5}$$

$$Sh = 2 + 0.6Gr^{1/4}Sc^{1/3} \tag{6}$$

$$Gr = \frac{L^3 g(\Delta\rho/\rho)}{\nu^2} \tag{7}$$

$$Sc = \frac{\nu}{D} \tag{8}$$

where Sh = Sherwood number, Gr = Grashof number, Sc = Schmidt number, D = diffusion coefficient, L = characteristic length (diameter of particle), $\Delta\rho/\rho$ = fractional density change based on density of fluid and solid particle, υ = kinematic viscosity of fluid. Here, k_m represents the mass transfer coefficient of the reactant through the fluid film around the suspended particle due to natural convection.

The first order dependence of k_{ss} on chloride ion concentration (at $[Cl^-] < 0.5$ mol.dm^{-3}) can be used to determine the value of k_B in Eq. 1. The y-intercept of line (e) corresponding to Y = Cl^- in Fig. 8a represents:

$$\log\left(\frac{bk_B}{r_o\rho}\right) = -6.96 \tag{9}$$

For pure covellite of density = 4.6 g cm^{-3} (Kelly and Spottiswood, 1997), particle diameter = 19 x 10^{-6} m and molar masses of Cu = 63.6 $g.mol^{-1}$, S = 32.1 $g.mol^{-1}$, the value of $r_o\rho_{Cu}$ is 0.31 $mol.m^{-2}$. The substitution of these values, and the value of b = 1 based on reaction R15 in Table 1 in Eq. 10, gives an experimental value of k_B = 3.3. 10^{-6} m s^{-1} for the intrinsic rate constant. The diffusion coefficients of H_3O^+, Cl^- and O_2 at 25°C are all close to 2. 10^{-9} m^2 s^{-1} (Marcus, 1997). The use of D = 6. 10^{-9} m^2 s^{-1} at 85°C leads to a calculated value of k_m = 1.10^{-3} m s^{-1} based on Eqs. 5-8 (Table 5). The experimental value of k_B (~10^{-6} m s^{-1}) for the surface reaction (Eq. 10) is three orders of magnitude lower than the estimated value of k_m from Eqs. 5-8 (~10^{-3} ms^{-1}). This shows that the approximately first order dependence of k_{ss} of covellite on the concentration of chloride ions is due to the involvement of chloride in the surface reaction, rather than mass transport to the surface. This situation is similar to the previously reported results (Raschman and Fedorockova, 2006) in which the intrinsic rate constant for the surface reaction for the dissolution of periclase in hydrochloric acid was three orders of magnitude lower than the calculated mass transfer coefficient of acid.

The initial rate of the surface reaction per unit surface area can be expressed by Eq. 10 (Senanayake, 2007a). According to Fick's first law, the flux of A is expressed by Eq. 11. At steady state, reagent A reacts with solid B at the same rate as it arrives at the surface. This leads to Eq. 12 for the rate of surface reaction at steady state (Cs = 0). The use of k_m calculated from Eqs. 5-8 allows the comparison of estimated rate (Eq. 12) with measured rate (Eq. 10).

$$R = k_{ss} r_o \rho \quad (10)$$

$$\text{Flux} = k_m(C_A - C_s) \quad (11)$$

$$R = b\, k_m C_A \quad (R \text{ and flux in mol } m^{-2}\, s^{-1}) \quad (12)$$

Line (d) in Fig.10 shows the effect of concentration of dissolved oxygen on the experimental rate of dissolution of covellite. The results for chalcocite from previous studies (Table 4, Fig. 8b) are also shown by line (a) in Fig. 10 for comparison. In the case of chalcocite, the estimated and measured rates closely agree, especially if a value of b = 1 was used, indicating that at steady state the surface reaction is controlled by the oxygen mass transfer. However, in the case of covellite, the measured rates are one or two orders of magnitude lower than the estimated rates. The fact that the rate is proportional to $(C_{O2})^{0.45}$ and $(C_{Cl}^{-})^{1}$ based on the slopes of lines d and e in Fig. 8a, respectively, indicates the importance of considering a mechanism which involves both these species in the surface reaction.

11. Electrochemical evidence for chloride assisted surface reaction

Previous studies have shown that a comparison of the predicted potentials of various redox couples with the peak potentials of voltammograms of relevant minerals/metals can be used to examine the nature of interim species formed on the surface during leaching reactions (Hillrichs and Bertram, 1983; Wadsworth and Zhu, 2005, Senanayake, 2008a). The lines in Fig. 11 show the calculated E^{o} values for the formation of elemental sulfur and different copper species including chloride, oxides and hydroxides and selected sulfur species during covellite oxidation as a function of temperature.

Hillrichs and Bertram (1983) noted that the anodic dissolution/decomposition of CuS will proceed only when the current densities are low and the rate of oxidation reaction CuS→ CuO/S becomes low compared that of CuS→ Cu^{2+}/S. This was consistent with the non-passivated CuS decomposition at very low current densities

reported by Peters (1977b). In the reported voltammogram for the anodic oxidation of covellite in 0.2 mol.dm^{-3} H_2SO_4/NaCl at 25^{o}C (Miki and Nicol, 2008a), the two peak potentials at 0.62 V and 0.74 V are consistent with the calculated potentials (reactions R39 and R44 in Table 2 and "a" in Fig. 11). The two couples represented by these potentials are CuS/$CuCl^{+}$, S and CuS/$Cu_2(OH)_3Cl$, S, respectively. The lower peak potential of 0.62 V is also in excellent agreement with the E^{o} value of 0.62 V relevant to Cu(OH)Cl calculated in the present study (reaction R39 in Table 2 and "b" in Fig. 11). Moreover, the calculated values of Eh for these two redox couples at 25^{o}C based on the Nernst equation, E^{o} in Table 2, and the two concentrations 0.2 mol dm^{-3} Cl^{-}, and 0.2 mol dm^{-3} H^{+}; assuming the dissociation $H_2SO_4 = H^{+} + HSO_4^{-}$ (Fig. 6) and unit activity coefficients are 0.721 and 0.601 V respectively. These values are close to the measured peak potentials reported by Miki and Nicol (2008a) indicating the possibility of precipitation of these solids under the specified conditions. In contrast, the E^{o} values of other redox couples of interest: CuS/$CuCl_2^{-}$,S (0.792 V), CuS/CuCl,S (0.704 V) and CuS/CuCl, $H_2S_2O_3$ (0.539 V) differ from the measured values noted above and in Fig.11. The observed increase in anodic peak currents with increasing chloride concentration also supports the involvement of chloride ions in the rate controlling step. The beneficial effect of chloride ions upon anodic oxidation of covellite in a sulfate system can be rationalised on the basis of reactions R48-R50 in Table 2, where the sum of reactions R48-R50 and R35 gives the overall oxidation reaction R16. Thus, the formation of Cu(OH)Cl (reaction R26) can be considered as the rate controlling step for covellite leaching in oxygenated sulfuric acid-chloride solutions.

12. Surface reaction mechanism of covellite leaching

The thermodynamically favoured reactions between dissolved oxygen and covellite expressed by R13-R14 in Table 1 at zero chloride concentration are expected to be very slow to yield very low copper extraction from CuS even in 0.5 mol.dm^{-3} H_2SO_4 at 90^{o}C, as observed in Fig. 2a. Thus, the beneficial role of chloride ions during the leaching of covellite by oxygen can be rationalised according to the anion-influenced adsorption-reaction-desorption mechanism via Cu(SH)(Cl) and Cu(OH)(Cl), described by reactions R24-R29 in Table 1. Relevant mathematical expressions are described in Appendix A.

Reactions R26 and R27 would lead to the formation of a more porous surface, compared to the tight passivating surface formed in the absence of chloride. The formation of Cu(I) chloro complexes in oxygen deficient chloride slurry systems, reported by Cheng and Lawson (1991b) is possible via CuCl produced according to reaction R27. Likewise, the formation of both sulfur and sulfate can be related to the interim species $H_2S_2O_2$ in side reactions R30-32 as well as other species such as thiosulfate (Ho and Muir, 2006). The interim product CuCl can be dissolved as $CuCl_n^{-(n-1)}$ in excess chloride and/or be oxidized to Cu(II) salts by oxygen (R28). The non-existence of thiosulfurous acid ($H_2S_2O_2$) and dithionous acid ($H_2S_2O_4$) in the free molecular state (Greenwood and Earnshaw, 1984) indicates the possible conversion of only a small percentage of sulfide to sulfate via these unstable intermediates and side reactions, or other species such as thiosulfate, as observed by Cheng and Lawson (1991b). Further work is essential to compare and contrast the leaching behaviour of CuS and $CuFeS_2$.

13. Summary and concluding remarks

The leaching results of synthetic covellite in the initial 15-30 minutes follow a shrinking sphere kinetic model, indicating that the rate is controlled by a chemical reaction at the surface. Rate constants correspond to a half order reaction with respect to dissolved oxygen concentration, but zero order with respect to hydrogen ions at high acid concentrations. Chloride ions are involved in the surface reaction as revealed by the first order dependence of the apparent rate constant on chloride ion concentration in the range 0.02-0.25 mol dm^{-3}. However, the calculated mass transfer coefficient of species such as oxygen and chloride ions (k_m ~10^{-3} m s^{-1}) is three orders of magnitude larger than the intrinsic rate constants based on a shrinking sphere kinetic model (k_B ~10^{-6} m s^{-1}). This also supports the view that chloride ions are involved in the rate controlling surface chemical reaction. The calculated standard reduction potentials compare reasonably well with the reported peak potentials of linear sweep voltammograms of covellite. This supports the proposed surface reaction mechanism via the formation of mixed-ligand complexes, in the form of adsorbed or dissolved species.

Appendix A

Reaction of CuS in oxygenated acid in the presence of chloride ions

1. $CuSH^+ + Cl^- \rightleftharpoons Cu(SH)(Cl)_{ads}$ (adsorption)
   (1-θ) θ
2. $Cu(SH)(Cl) + 0.5O_2 \xrightarrow{k} S + Cu(OH)(Cl)_{ads}$ (or $0.5H_2S_2O_2 + CuCl$)
   (rate controlling)
3. $Cu(OH)(Cl)_{ads} + HSO_4^- = Cu(SO_4)^0 + H_2O + Cl^-$
4. $CuS + H_2SO_4 + 0.5O_2 = Cu(SO_4)^0 + H_2O$ (overall)

$$K = \frac{\theta}{(1-\theta)][Cl^-]}$$

$$\theta = \frac{K[Cl^-]}{1+K[Cl^-]}$$

$$R = k\,\theta[O_2]^a = \frac{kK[Cl^-][O_2]^a}{1+K[Cl^-]}$$

θ = fraction of CuS surface that undergoes reaction with O_2
K = equilibrium constant for the adsorption equilibrium in reaction (1)
k = rate constant
a = reaction order with respect to O_2
R = reaction rate
At high concentrations of Cl^- it may be assumed that $1 << K[Cl^-]$. This leads to the expression $R = k[O_2]^a$, which explains the chloride independent rates at higher chloride concentrations.

References

Berezowsky, R. Trytten, L., 2002. Commercialization of the acid pressure leaching of chalcopyrite. ALTA Copper 7 Forum, Perth. ALTA Metallurgical Services, Melbourne. 40 pp.

Bertram, R., Hillrichs, E., 1981. Stimulation of the dissolution of copper sulfide electrodes. J. Electroanalytical Chemistry. 129, 365-368.

Beverskog, B., Puigdomenech, I., 1997. Revised Porbaix diagrams for copper at 25 to 300^{o}C. J. Electrochemical Soc., 144, 3476-3483.

Brown, J.A., Papangelakis, G., 2005. Interfacial studies of liquid sulphur during aqueous pressure oxidation of nickel sulphide. Minerals Engineering. 18, 1378-1385.

Buckley, A., Woods, R., 1984. An X-ray photoelectron spectroscopic study of the oxidation of chalcopyrite. Australian J. Chemistry 37, 2403-2413.

Carneiro, M.F.C., Leao, V.A., 2007. The role of sodium chloride on surface of chalcopyrite leached with ferric sulfate. Hydrometallurgy 87, 73-82.

Cheng, Y.C., Lawson, F., 1991a. The kinetics of leaching chalcocite in acidic oxygenated sulphate-chloride solutions. Hydrometallurgy 27, 249-268.

Cheng, Y.C., Lawson, F., 1991b. The kinetics of leaching covellite in acidic oxygenated sulphate-chloride solutions. Hydrometallurgy 27, 269-284.

Cordoba, E.M., Munoz, J.A., Blazquez, M.L., Gonzalez, F., Ballester, A., 2008a. Leaching of chalcopyrite with ferric ion. Part I: General aspects. Hydrometallurgy 93, 81-87.

Cordoba, E.M., Munoz, J.A., Blazquez, M.L., Gonzalez, F., Ballester, A., 2008b. Leaching of chalcopyrite with ferric ion. Part II: Effect of redox potential. Hydrometallurgy 93, 88-96.

Crundwell, F.K., 1988. The influence of the electronic structure of solids on the anodic dissolution and leaching of semi-conducting sulphide minerals. Hydrometallurgy 21, 155-190.

Cussler, E.L., 1997. Diffusion: Mass Transfer in Fluid Systems. Cambridge University Press.

Defreyne, J., Grieve, W., Jones, D.L., Mayhew, K., 2006. The role of iron in CESL process. In: Dutrizac, J.E., Riveros, P.A. (Eds.), Iron Control Technologies (Proc. 3rd International Symposium). Canadian Institute of Mining, Metallurgy, and Petroleum, Montreal, pp. 205-220.

Deng, T., Lu, Y., Wen, Z., Liu, D., 2001. Oxygenated chloride-assisted leaching of copper residue. Hydrometallurgy 62, 23-30.

Dreisinger, D. 2006. Copper leaching from primary sulfides: Options for biological and chemical extraction of copper. Hydrometallurgy 83, 10-20.

Dutrizac, J.E., 1992. The leaching of sulphide minerals in chloride media. Hydrometallurgy 29, 1-45.

Ferron, C.J., Fleming, C.A., O'Kane, P.T., Dreisinger, D., 2002. High temperature chloride assisted leach process to extract simultaneously Cu, Ni, Au and PGM's from various feedstocks. In Chloride Metallurgy 2002 (Eds. Peek, E., Van Weert, G.) Canadian Institute of Mining, Metallurgy, and Petroleum, Montreal, pp.11-28.

Fisher, W.W., Flores, F.A., Henderson, J.A., 1992. Comparison of chalcocite dissolution in the oxygenated, aqueous sulfate and chloride systems. Minerals Engineering, 5, 817-834.

Flett, D.S., 2002. Chloride hydrometallurgy for complex sulphides: a review. In Chloride Metallurgy 2002 (Eds. Peek, E., Van Weert, G.) Canadian Institute of Mining, Metallurgy, and Petroleum, Montreal pp 255-276.

Gerlach, J., Kuzeci, E., 1983. Application of carbon paste electrodes to elucidate hydrometallurgical dissolution processes with special regard to chalcocite and covellite. Hydrometallurgy 11, 345-361.

Goh, S.W., Buckley, A.N., Lamb, R.N., 2006. Copper(II) sulfide? Minerals Engineering 19, 204-208.

Grewal, I., Dreisinger, D.B., Krueger, D., Tyroler, P.M., Krause, E., Nissen, N.C., 1992. Total oxidative leaching of Cu_2S-containing residue at INCO s copper refinery: laboratory studies on the reaction pathways. Hydrometallurgy 29, 319-333.

Greenwood, N.N., Earnshow, A., 1984. Chemistry of the Elements. Pergamon Press, New York.

Grizo, A., Pacovic, N., Poposka, F., Koneska, Z., 1982. Leaching of a low-grade chalcocite-covellite ore containing iron in sulphuric acid: The influence of pH and particle size on the kinetics of copper leaching. Hydrometallurgy, 8, 5-16.

Hackl, R.P., 1995. Passivation of chalcopyrite during oxidative leaching in sulfate media. Hydrometallurgy 39, 25-48.

Haywood, R.W., 1990. Thermodynamic Tables in SI Units**.** Cambridge University Press, UK.

Herreros, O., Quiroz, R., Longueira, H., Fuentes, G., Vinals, J., 2006. Leaching of djurleite in Cu^{2+}/Cl^- media. Hydrometallurgy 82, 32-39.

Herreros, O., Vinals, J., 2007. Leaching of sulfide copper ore in $NaCl-H_2SO_4-O_2$ media with acid pre-treatment. Hydrometallurgy 89, 260-268.

Hillrichs, E., Bertram, R., 1983a. Anodic dissolution of copper sulphides in sulphuric acid solutions. I. The anodic decomposition of $Cu_{2-x}S$. Hydrometallurgy 11, 181-193.

Hillrichs, E., Bertram, R., 1983b. Anodic dissolution of copper sulphides in sulphuric acid solutions. II. The anodic decomposition of CuS. Hydrometallurgy 11, 195-206.

Hirato, T., Hiai, H., Awakura, Y., Majima, H., 1989. The leaching of sintered CuS disks with ferric chlorides. Metallurgical Transactions. 20B, 485-491.

Ho, E., 1996. Ph. D. Thesis, Murdoch University, Perth, Australia.

Hogfeldt, E., 1982. Stability Constants of Metal-Ion Complexes, 2nd Supplement, IUPAC Chemical data series No. 2, Part A, Inorganic ligands, Oxford, Pergamon.

Ilkuchi, M.O., Yoozbashizadeh, H., Safarzadeh, M.S., 2007. The effect of additives on anode passivation in electrorefining of copper. Chemical Engineering Processing 46, 757-763.

Johnson, G.D., Streltsova, N., 1999. Method for the processing of copper minerals. US Patent 3,856,913, December 24, 1974.

Kelly, E.G., Spottiswood, D.J., 1997. Introduction to Mineral Processing, Australian Mineral Foundation.

Klauber, C., Parker, A., van Bronswijk, W., Watling, H., 2001. Sulphur speciation of leached chalcopyrite surfaces as determined by X-ray photoelectron spectroscopy. Intl. J. Mineral Processing 62, 65-94.

Klauber, C., 2008. A critical review of the surface chemistry of acidic ferric sulphate dissolution of chalcopyrite with regards to hindered dissolution. Intl. J. Mineral Processing. 86, 1-17.

Kinnunen, P.H.-M., Puhakka, J.A., 2004. Chloride-promoted leaching of chalcopyrite concentrate by biologically-produced ferric sulfate. J. Chemical Technology and Biotechnology. 79, 830-834.

Koch, D.F.A., McIntyre, R.J., 1976. The application of reflectance spectroscopy to a study of the anodic oxidation of cuprous sulphides. J.Electroanalytical Chemistry. 71, 285-296.

Lazaro, I., Nicol, M.J., 2006. A rotating ring-disk study of the initial stages of the anodic dissolution of chalcopyrite in acidic solutions. J. Applied Electrochemistry 36, 425-431.

Lee, M.S., Nicol, M.J., Basson, P., 2008. Cathodic processes in the leaching and electrochemistry of covellite in mixed sulfate-chloride media. J. Applied Electrochemistry 38, 363-369.

Levenspiel, O., 1972. Chemical Reactions Engineering. Wiley, New York.

Liddicoat, J., Dreisinger, D., 2007. Chloride leaching of chalcopyrite. Hydrometallurgy 89, 323-331.

Lin, H.K., Sohn, H.Y., 1987. Mixed-control kinetics of oxygen leaching of chalcopyrite and pyrite from porous primary ore fragments. Metallurgical Transactions 18B, 497-503.

Lotens, J.P., Wesker, E., 1987. The behaviour of sulphur in the oxidative leaching of sulphide minerals. Hydrometallurgy 18, 39-54.

Lu, Z.Y., Jeffrey, M.I., Zhu, Y., Lawson, F., 2000a. Studies of pentlandite leaching in mixed oxygenated acidic chloride-sulphate solutions. Hydrometallurgy 56, 63-74.

Lu, Z.Y., Jeffrey, M.I., Lawson, F., 2000b. The effect of chloride ions on the dissolution of chalcopyrite in acidic solutions. Hydrometallurgy 56, 189-202.

Lundstrom, M., Aromaa, J., Forsen, O., Hyvarinen, O., Barker, M.H., 2005. Leaching chalcopyrite in cupric chloride solution. Hydrometallurgy 77, 89-95.

Majima, H., Awakura, Y., Hirato, T., Tanaka, T., 1985. The leaching of chalcopyrite in ferric chloride and ferric sulfate solutions. Canadian Metallurgy Quarterly. 24, 283-291.

Majima, H., Awakura, Y., Yazaki, T., Chiakamori, Y., 1980. Acid dissolution of cupric oxide. Metallurgical Transactions. 11B, 209-214.

Majima, H., 1995. Importance of fundamental study in hydrometallurgy. Metallurgical and Materials Transactions 26B, 1109-1122.

Marcus, Y., 1997. Ion Properties. Marcel Dekker, New York.

Mao, M.H., Peters, E., 1983. Acid pressure leaching of chalcocite. In: Osseo-Asare, K., Miller, J.D. (Editors), Hydrometallurgy: Research, development and Plant Practice. Met..Soc. AIME, Warrendale, PA, pp. 243-260.

McCarthy, A.J., Coleman, R.G., Nicol, M.J., 1998. The mechanism of the oxidative dissolution of colloidal gold in cyanide media. J. Electrochemical Society., 145, 408-414.

McDonald, G.W., Langer, S.H., 1983. Cupric chloride leaching of model sulfur compounds for simple copper ore concentrates. Metallurgical Transactions. 14B 559-570.

McDonald, R.G., Muir, D.M., 2007a. Pressure oxidation leaching of chalcopyrite Part I: Comparison of high and low temperature reaction kinetics and products. Hydrometallurgy 86, 191-205.

McDonald, R.G., Muir, D.M., 2007b. Pressure oxidation leaching of chalcopyrite Part II: Comparison of medium temperature kinetics and products and effect of chloride ion. Hydrometallurgy 86, 206-220.

Mikhlin, Y.L., Tomashevich, Y.V., Asanov, I.P., Okotrub, A.V., Varnek, V.A., Vyalikh, D.V., 2004. Spectroscopic and electrochemical characterization of the surface layers of chalcopyrite ($CuFeS_2$) reacted in acidic solutions. Applied Surface Science 225, 395-409.

Miki, H. and Nicol, M.J., 2008a. Synergism in the oxidation of covellite and pyrite by iron(III) and copper(II) ions in chloride solutions. In Hydrometallurgy 2008. Proc. 6th International Symposium (Eds. Young, C.A., Taylor, P.R., Anderson, C.G., Choi, Y.) SME, Littleton, pp.646-652, and references therein.

Miki, H. and Nicol, M.J., 2008b. The kinetics of the copper-catalysed oxidation of iron(II) in chloride solutions. In Hydrometallurgy 2008 (Proc. 6th International Symposium; Eds. Young, C.A., Taylor, P.R., Anderson, C.G., Choi, Y.) SME, Littleton, pp.971-979.

Moats, M.S., Hiskey, J.B., 2000. The role of electrolyte additives on passivation behaviour during copper electrorefining. Canadian Metallurgical Quarterly 39, 297-306.

Muir, D.M., 2002. Basic principles of chloride hydrometallurgy. In Chloride Metallurgy 2002 (Eds. Peek, E., Van Weert, G.) Canadian Institute of Mining, Metallurgy and Petroleum, Montreal pp 255-276.

Muir, D.M., 2009. Personal Communications.

Muir, D.M., Ho, E., 2006, process review and electrochemistry of nickel sulphides and nickel mattes in acidic sulphate and chloride media. Mineral Processing and Extractive Metallurgy, 115, 57-65 .

Muir, D.M., Parker, A.J., Filmer, A.O., Wadley, L.G.B., Clare, B.W., 1981. Formation of sulfur from the ammonia/oxygen leach of copper and nickel sulfides. Proceedings Hydrometallurgy'81. Society of Chemical Industry, London, paper B3.

Nicol, M.J., 2007. The mechanisms of the leaching of sulphide minerals – a reappraisal. Unpublished paper presented at the 7th Meeting of Southern Hemisphere on Mineral Technology/XXII held in Ouro Preto, Minas Gerais, Brazil, November 20-24, 2007 (personal communication).

Nicol, M.J., Lazaro, I., 2003. The role of non-oxidative processes in the leaching of chalcopyrite. Hydrometallurgy of Copper 1: leaching and process development. Ed. Riveros, P.A., Dixon, D., Dreisinger, D.B., Menacho, J., Canadian Institute of Mining, Metallurgy and Petroleum, Montreal pp. 367-381.

Parker, A.J., Paul, R.L., Power, G.P., 1981. Electrochemical aspects of leaching copper from chalcopyrite in ferric and cupric salt solutions. Australian. J. Chemistry. 34, 13-34.

Parker, G., Woods, R., Hope, G.A., 2003. Raman investigation of sulfide leaching. Hydrometallurgy 2003, TMS, Warrendale, pp. 447-460.

Parker, G.K., Hope, G.A., Woods, R., 2008a. Raman investigation of chalcopyrite oxidation. Colloids and Surfaces A: Physicochemical and Engineering Aspects 318, 160-168.

Parker, G.K., Hope, G.A., Woods, R., 2008b. Gold-enhanced Raman observation of chalcopyrite leaching. Colloids and Surfaces A: Physicochemical and Engineering Aspects 325, 132-140.

Peacey, J., Guo, X.J., Robles, E., 2003. Copper hydrometallurgy – Current status, preliminary economics, future directions, and positioning versus smelting. Hydrometallurgy of Copper 1: leaching and process development. Ed. Riveros, P.A., Dixon, D., Dreisinger, D.B., Menacho, J., Canadian Institute of Mining, Metallurgy and Petroleum, Montreal pp. 205-222.

Pearson, R.G., 1973. Hard and Soft Acids and Bases. Stroudsburg, PA: Dowden, Hutchinson & Ross, 1973.

Peters, E., 1976a. The electrochemistry of sulphide minerals. Proceedings of 4th Australian Electrochemistry Conference, RACI, Melbourne. pp. 267-290.

Peters, E., 1976b. Direct leaching of sulphides: Chemistry and applications. Metallurgical Transactions. 7B, 505-517.

Peters, E., 1977a. Applications of chloride hydrometallurgy to treatment of sulphide minerals. Proc. Symposium on Chloride Hydrometallurgy, Benelux Metallurgie, Brussels, pp. 1-37.

Peters, E., 1977b. In: Trends in Electrochemistry. Ed. Bockris, J.O.M., Rand, D.A.F., Welch, R.J., Plenum Press, New York, p. 267.

Provis, J. L., van Deventer, J. S. J., Rademan, J. A. M., Lorenzen, L., 2003. A kinetic model for the acid-oxygen pressure leaching of Ni–Cu matte. Hydrometallurgy 70, 83-99.

Rademan, J.A.M., Lorenzen, L., van Deventer, J.S.J., 1999. The leaching characteristics of Ni-Cu matte in the acid-oxygen pressure leach process at Impala Platinum. Hydrometallurgy 52, 231-252.

Raschman, P., Fedorockova, A., 2006. Dissolution of periclase in excess of hydrochloric acid: Study of inhibiting effect of acid concentration on the dissolution rate. Chemical Engineering Journal 117, 205-211.

Ruiz, M.C., Honores, S., Padilla, R., 1998. Leaching kinetics of digenite concentrate in oxygenated chloride media at ambient pressure. Metallurgical and Materials Transactions 29B, 961-969.

Ruiz, M.C., Abarzua, E., Padilla, R., 2007. Oxygen pressure leaching of white metal. Hydrometallurgy 86, 131-139.

Sabba, N., Akretche, D-E., 2006. Selective leaching of copper ore by an electro-membrane process using ammonia solutions. Minerals Engineering 19, 123-129.

Senanayake, G., 2007a. Review of rate constants for thiosulphate leaching of gold from ores, concentrates, and flat surfaces: Effect of host minerals and pH. Minerals Engineering 20, 1-15.

Senanayake, G., 2007b. Review of theory and practice of measuring proton activity and pH in concentrated chloride solutions and application to oxide leaching. Minerals Engineering 20, 634-645.

Senanayake, G., 2007c. Chloride assisted leaching of chalcocite by oxygenated sulphuric acid via Cu(II)-OH-Cl. Minerals Engineering 20, 1075-1088.

Senanayake, G., 2008a. A review of effect of silver, lead, sulfide and carbonaceous matter on gold cyanidation and mechanistic interpretation. Hydrometallurgy 90, 46-75.

Senanayake, G., 2008b. Erratum to Chloride assisted leaching of chalcocite by oxygenated sulphuric acid via Cu(II)-OH-Cl. Minerals Engineering 21, 421.

Senanayake, G., Muir, D.M., 1988. Speciation and reduction potentials of metal ions in concentrated chloride and sulphate solutions relevant to processing base metal sulfides. Metallurgical Transactions 19B, 37-45.

Senanayake, G., Muir, D.M., 2003. Chloride processing of metal sulphides: Review of fundamentals and applications. Proc. Hydrometallurgy 2003, Eds Young C.A et al; TMS, Warrendale, pp. 517-531.

Sequeira,C.A.C., Santos, D.M.F., Chen, Y., Anastassakis, G., 2008. Chemical metathesis of chalcopyrite in acidic solutions. Hydrometallurgy 93, 135-140.

Sillen, L.G., Martell, A.E., 1964. Stability Constants of Metal Complexes. In: Chemical Society Special Publication, vol. 17, and 26. Chemical Society, London.

Subramanian, K.N., Ferrajuolo, R., 1976. Oxygen pressure leaching of Fe-Ni-Cu sulfide concentrates at 110 ^{o}C – Effect of chloride addition. Hydrometallurgy 2, 117-125.

Sullivan, J.D., 1933. Chemical and physical features of copper leaching. Transactions American Inst. Mining and Metallurgy, 106, 515-547.

Tromans, D., 1998. Temperature and pressure dependent solubility of oxygen in water: a thermodynamic analysis. Hydrometallurgy 48, 327-342.

Ueda, H., Nohara, M., Kitazawa, K., Takagi, H., Fujimori, A., Mizokawa, T., Yagi, T., 2002. Copper pyrites CuS_2 and $CuSe_2$ as anion conductors. Physical Review B65, 155104.

Viramontes-Gamboa, G., Rivera-Vasquez, B.F., Dixon, D.G., 2007. Experimental predictions of the potential range to leach chalcopyrite in acidic ferric sulfate media. In: The J.E. Dutrizac International Symposium on Copper Hydrometallurgy. Ed. Riveros, P.A., Dixon, D.G., Dreisinger, D.B., Collins, M.J., Canadian Institute of Mining, Metallurgy, and Petroleum, Toronto pp. 269-284.

Wadsworth, M.E., Zhu, X., 2005. Kinetics of enhanced gold dissolution: activation by dissolved lead. In:Young, C.A., Kellar, J.J., Free,M.L., Drelich, J., King, R.P. (Eds.), Innovation in Natural Resources Processing. Proceddings J.D. Miller Symposium, SME, Littleton, pp. 3–10.

Wagman, D.D., Evans, W.H., Parker V.B., Shuman, R.H., Halow, I., Balley, S.M., Churney, K.L., Nuttall, R.L., 1982. The NBS tables of chemical thermodynamic properties. J. Physical Chemistry Ref. Data 11 (Suppl. 2), 2-119.

Watling, H.R., 2006. The bioleaching of sulphide minerals with emphasis on copper sulphides – A review. Hydrometallurgy 84, 81-108.

Winand, R., 1991. Chloride hydrometallurgy. Hydrometallurgy 27, 285-316.

Yin, Q., Kelsall, G.H., Vaughan, D.J., England, K.E.R., 1995. Atmospheric and electrochemical oxidation of the surfcae of chalcopyrite ($CuFeS_2$). Geochimica et Cosmochimica Acta 59, 1091-1100.

Young, C.A., Dahlgren, E.J., Robins, R.G., 2003. The solubility of copper sulfides under reducing conditions. Hydrometallurgy 68, 23-31.

Figure Captions

Fig. 1.
(a) Potential-log[Cl^-] diagrams for iron-copper-chloride-water system at 25 ^oC and 0.1 mol dm^{-3} metal ions (Senanayake and Muir, 2003); (b) potential-pH diagram for chalcocite and covellite leaching by oxygen at 25^{o}C and 90^{o}C and unit activities based on Outukumpu HSC 6.1 software (dashed lines represents O_2/H_2O and H_2/H^+ couples).

Fig. 2.
Effect of sodium chloride on copper leaching from (a) covellite by oxygen, 13 μm, 90^{o}C, 0.5 mol dm^{-3} H_2SO_4; (b) chalcocite by oxygen, 31 μm, 85^{o}C, 0.5 mol dm^{-3} H_2SO_4 (data from Chang and Lawson, 1991a,b).

Fig. 3.
Linear correlation between equilibrium constants for complexation and precipitation of M(II): (a) Cu(II)-Pb(II) at 25^{o}C; (b) Cu(II)-Fe(II) at 25^{o}C and 90^{o}C (data from Table 3 Young et al., 2003 and HSC 6.1 database).

Fig. 4
Softness of cations and anions (Marcus, 1997).

Fig. 5
Effect of oxygen mole percent in the bubbling gas on $1-(1-X)^{1/3}$ during covellite leaching (D1-D4 described in Table 4, data from Cheng and Lawson, 1991b).

Fig. 6
Effect of sulfuric acid concentration on species distribution in 0.5 mol dm^{-3} NaCl+H_2SO_4 at 90 ^{o}C (Thermodynamic data from Hogfeldt, 1982)

Fig. 7
Effect of temperature on concentration of dissolved oxygen in water (Tromans, 1998).

Fig. 8
Log-log plots of k_{ss} versus reagent concentration (a) covellite: Y = O_2 (D1-D4), Y= Cl^- (E1-E4), Y = H^+ (F1-F4); (b) chalcocite; data from Table 4.

Fig.9
Arrhenius plots for the second stage leaching of chalcocite and initial leaching of covellite based on Eq. 4 (k_{ss} from Cheng and Lawson 1991a,b; dissolved oxygen concentration from Fig. 7).

Fig. 10
Correlation between dissolved oxygen concentration and measured (Eq. 10) or estimated (Eq. 12) rate data for chalcocite (85^{o}C) and covellite (90^{o}C) (see text).

Fig. 11
Effect of temperature on standard reduction potentials of covellite leaching products based on Outukumpu HSC 6.1 software.

Fig. 1
(a)

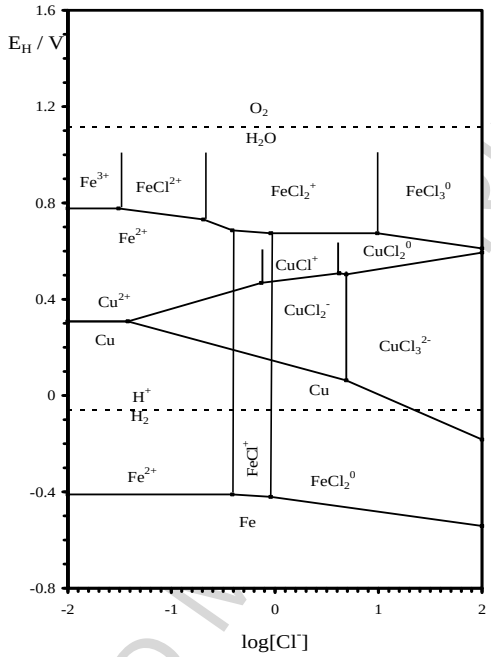

(b)

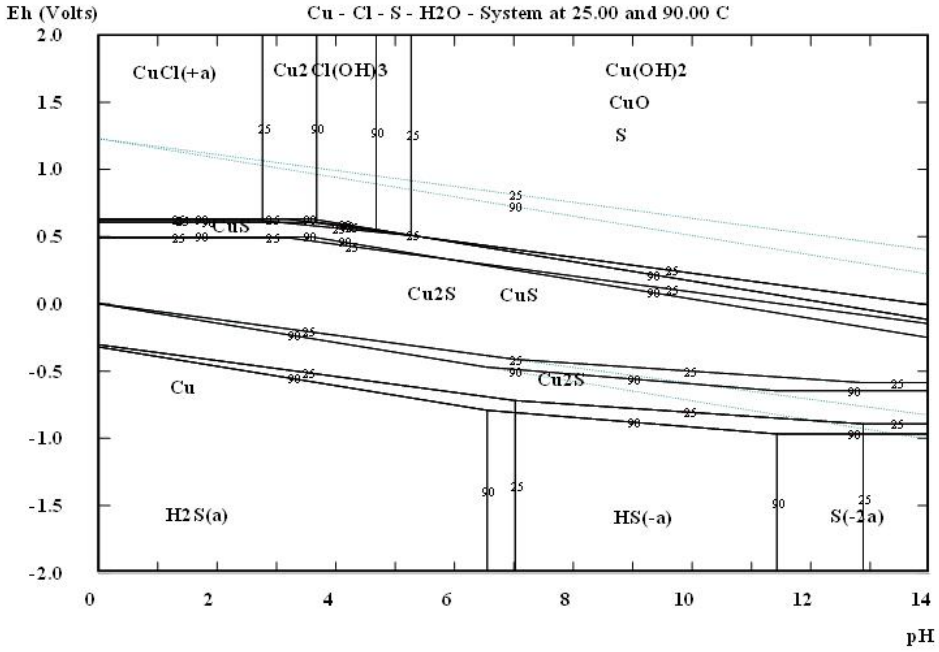

Fig. 1.
(a) Potential-log[Cl^-] diagrams for iron-copper-chloride-water system at 25 ^oC and 0.1 mol dm^{-3} metal ions (Senanayake and Muir, 2003); (b) potential-pH diagram for chalcocite and covellite leaching by oxygen at 25^oC and 90^oC and unit activities based on Outukumpu HSC 6.1 software (dashed lines represents O_2/H_2O and H_2/H^+ couples).

Fig. 2
(a)

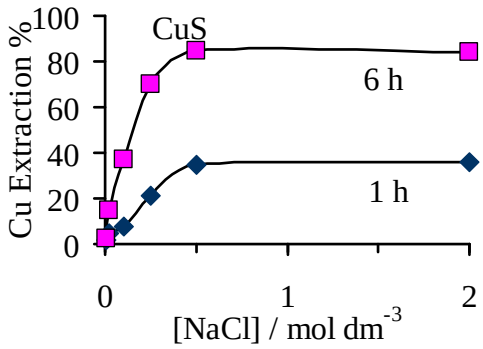

(b)

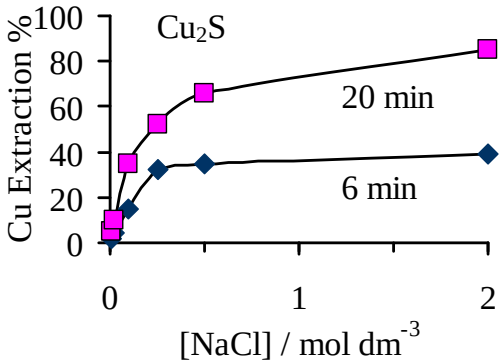

Fig. 2.
Effect of sodium chloride on copper leaching from (a) covellite by oxygen, 13 μm, 90°C, 0.5 mol dm^{-3} H_2SO_4; (b) chalcocite by oxygen, 31 μm, 85°C, 0.5 mol dm^{-3} H_2SO_4 (data from Chang and Lawson, 1991a,b).

Fig. 3
(a)

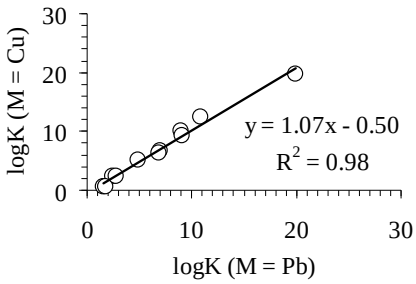

(b)

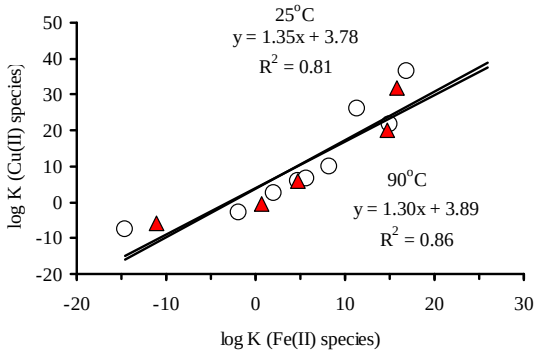

Fig. 3.
Linear correlation between equilibrium constants for complexation and precipitation of M(II): (a) Cu(II)-Pb(II) at 25°C; (b) Cu(II)-Fe(II) at 25°C and 90°C (data from Table 3 Young et al., 2003 and HSC 6.1 database).

Fig. 4

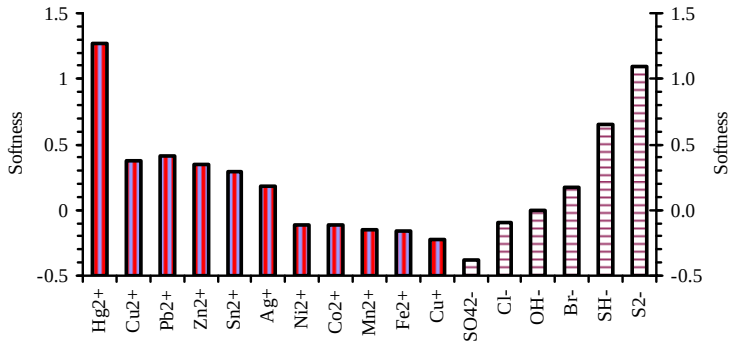

Fig. 4
Softness of cations and anions (Marcus, 1997).

Fig. 5

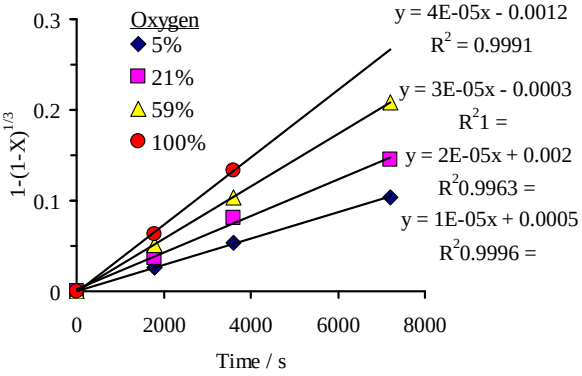

Fig. 5
Effect of oxygen mole percent in the bubbling gas on $1-(1-X)^{1/3}$ during covellite leaching (D1-D4 described in Table 4, data from Cheng and Lawson, 1991b).

Fig. 6

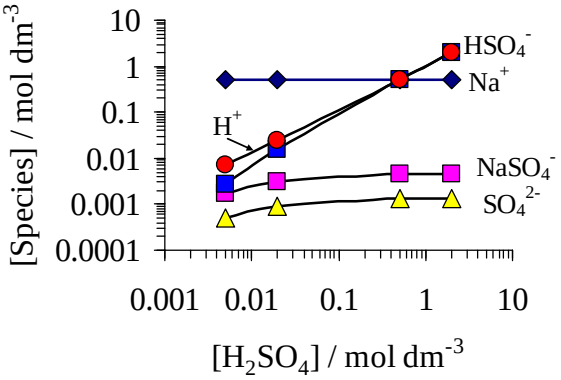

Fig. 6
Effect of sulfuric acid concentration on species distribution in 0.5 mol dm^{-3} NaCl+H_2SO_4 at 90 ^{o}C (Thermodynamic data from Hogfeldt, 1982)

Fig. 7

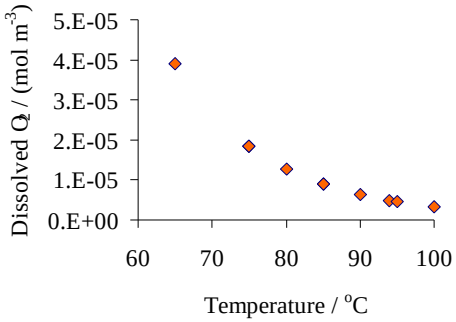

Fig. 7
Effect of temperature on concentration of dissolved oxygen in water (Tromans, 1998).

Fig.8
(a)

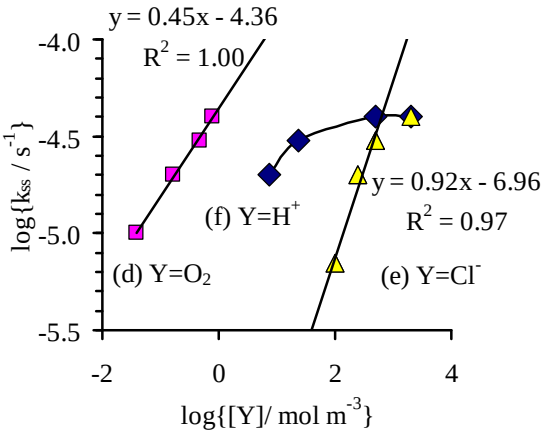

(b)

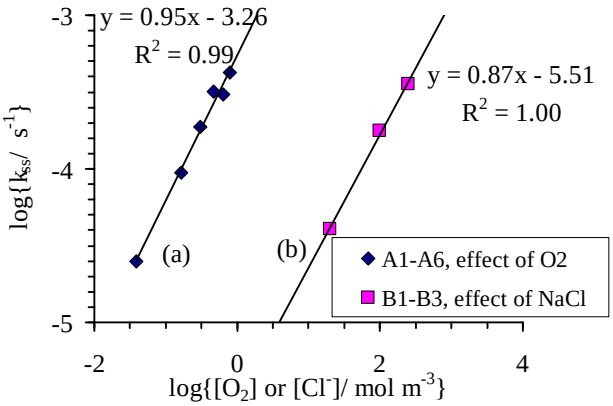

Fig. 8
Log-log plots of k_{ss} versus reagent concentration (a) covellite: Y = O_2 (D1-D4), Y= Cl^- (E1-E4), Y = H^+ (F1-F4); (b) chalcocite; data from Table 4.

Fig. 9

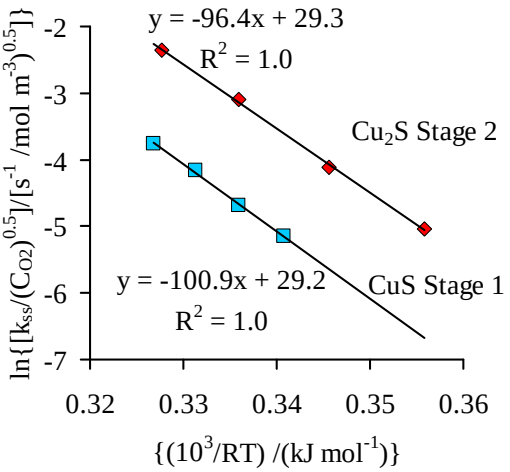

Fig.9
Arrhenius plots for the second stage leaching of chalcocite and initial leaching of covellite based on Eq. 4 (k_{ss} from Cheng and Lawson 1991a,b; dissolved oxygen concentration from Fig. 7).

Fig. 10

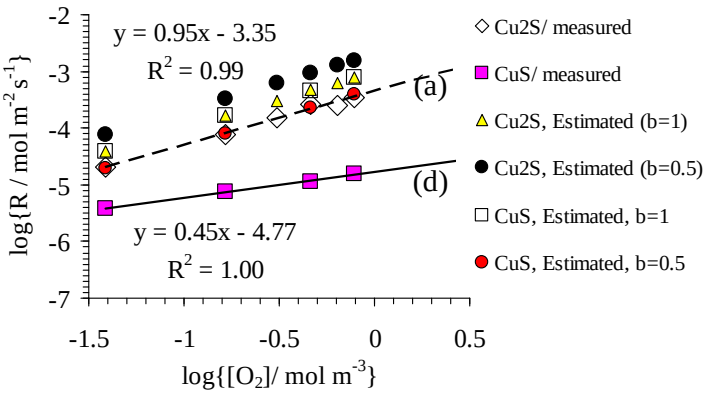

Fig. 10
Correlation between dissolved oxygen concentration and measured (Eq. 10) or estimated (Eq. 12) rate data for chalcocite (85°C) and covellite (90°C) (see text).

Fig.11

Peak potentials of anodic response of rotated electrodes of (a) covellite at ambient temperature in H_2SO_4 + NaCl (0.2 mol dm^{-3} each) (Miki and Nicol, 2008a) marked by asterisks ; (b) Calculated value for $CuS + H_2O + Cl^- = Cu(OH)Cl(s) + S + 2e^-$ (this work)

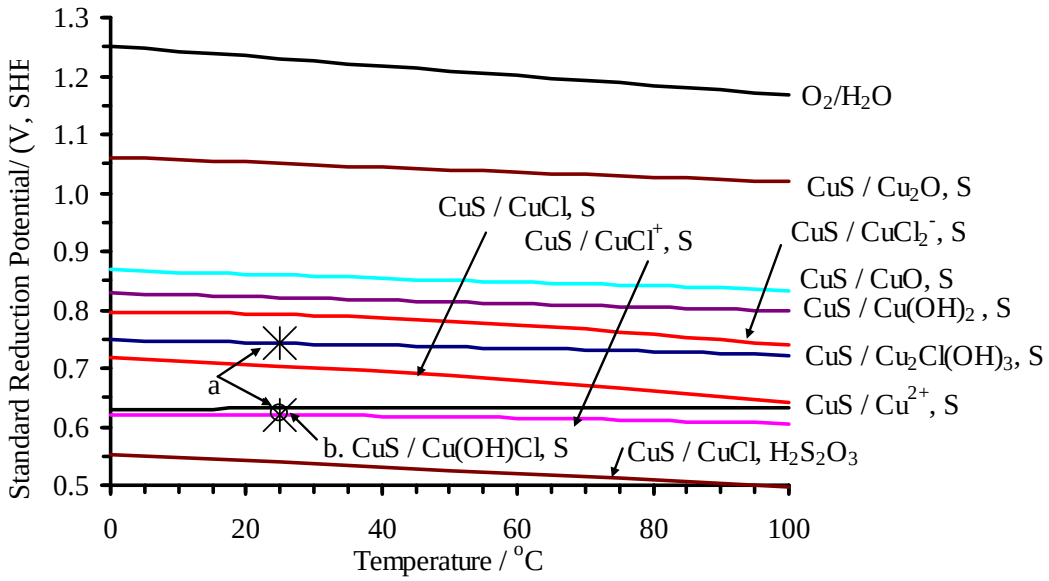

Fig. 11
Effect of temperature on standard reduction potentials of covellite leaching products based on Outukumpu HSC 6.1 software.

Table 1
Chemical reactions related to formation or oxygenated leaching of copper sulfides
(Some of these reactions were reported by Peters (1976a,b), Muir and Ho (2006); Rademan et al. (1999); Provis et al. (2003); Nicol and Lazaro (2003) (also see text), Equilibrium constants based on Outokumpu HSC 6.1 software).

Reaction	Equilibrium constant (K) 25°C	90°C
Leaching reactions which involve Cu_2S and CuS		
R1. $CuFeS_2 + 2H^+ = CuS + Fe^{2+} + H_2S$	$10^{-2.6}$	$10^{-2.4}$
R2. $CuFeS_2 + 2H^+ = 0.5Cu_2S + Fe^{2+} + H_2S + 0.5S$	$10^{-9.9}$	$10^{-8.5}$
R3. $Cu_2S + 2H^+ + 0.5O_2 = CuS + Cu^{2+} + H_2O$	10^{26}	10^{20}
R4. $Ni_3S_2 + 2H^+ = NiS + Ni^{2+} + H_2$	$10^{0.99}$	$10^{0.54}$
R5. $NiS + 2H^+ = Ni^{2+} + H_2S$	$10^{-2.08}$	$10^{-2.16}$
R6. $NiS + Cu^{2+} = CuS + Ni^{2+}$	10^{14}	10^{11}
R7. $Ni_3S_2 + 2Cu^{2+} = Cu_2S + NiS + 2Ni^{2+}$	10^{33}	10^{26}
R8. $Ni_3S_4 + 3Cu^{2+} + H_2O + 1.5O_2 = 3CuS + 3Ni^{2+} + 2H^+ + SO_4^{2-}$	10^{130}	10^{103}
Non-oxidative leaching of CuS		
R9. $CuS + 2H^+ = Cu^{2+} + H_2S$	$10^{-16.5}$	$10^{-13.8}$
R10. $CuS + H^+ + HSO_4^- = Cu(SO_4)^0 + H_2S$		
Leaching of Cu_2S by oxygen (first stage)		
R11. $Cu_2S + 0.5O_2 + H_2O = Cu(OH)_2 + CuS$	10^{20}	$10^{15.6}$
R12. $Cu_2S + 0.5O_2 + 2H^+ = Cu^{2+} + CuS + H_2O$	$10^{26.4}$	$10^{20.3}$
Leaching of CuS by oxygen		
R13. $CuS + 0.5O_2 + H_2O = Cu(OH)_2 + S$	$10^{15.5}$	$10^{11.8}$
R14. $CuS + 0.5O_2 + 2H^+ = Cu^{2+} + S + H_2O$	$10^{20.3}$	$10^{15.1}$
R15. $CuS + 0.5O_2 + 2H^+ + Cl^- = CuCl^+ + H_2O + S$		
R16. $CuS + 0.5O_2 + H^+ + HSO_4^- = Cu(SO_4)^0 + S + H_2O$		
Side reactions of CuS		
R17. $2CuS + 2H^+ + 2Cl^- + 1.5O_2 = 2CuCl + H_2S_2O_3$	$10^{37.2}$	$10^{30.2}$
R18. $2CuS + 2Cl^- + 2O_2 = 2CuCl + S + SO_4^{2-}$	$10^{56.2}$	$10^{44.5}$
Anion influenced non-oxidative leaching of CuS		
R19. $CuS + H^+ X^- = Cu(SH)(X)ads/aq$		
R20. $Cu(HS)(X)ads/aq + H^+ X^- = CuX_2 + H_2S$		
Anion influenced oxidative leaching of CuS		
R21. $CuS + H^+ X^- = Cu(SH)(X)ads/aq$		
R22. $Cu(HS)(X)ads/aq + 0.5O_2 = Cu(OH)(X)ads/aq + S$		
R23. $Cu(OH)(X)ads/aq + H^+ X^- = CuX_2 + H_2O$		
Chloride assisted leaching of CuS in sulfate medium		
R24. $CuS + H^+ = Cu(SH)^+(ads)$		
R25. $Cu(SH)^+(ads) + Cl^- = Cu(SH)(Cl)^0(ads/aq)$		
R26. $Cu(SH)(Cl)^0(ads/aq) + 0.5O_2(ads/aq) = Cu(OH)(Cl)^0(ads/aq) + S$		
R27. $2Cu(SH)(Cl)^0(ads/aq) = 2CuCl(ads/aq) + H_2S + S$		
R28. $2CuCl(ads/aq) + 0.5O_2 + H_2O = 2Cu(OH)Cl(ads/aq)$		
R29. $Cu(OH)(Cl)^0(ads/aq) + HSO_4^- = Cu(SO_4)^0 + Cl^- + H_2O$		

Possible side reactions

R30. $2Cu(SH)(Cl)^0(ads/aq) + O_2 = 2CuCl(ads/aq) + H_2S_2O_2$
R31. $H_2S_2O_2 + O_2 = H_2S_2O_4$
R32. $H_2S_2O_4 = H_2SO_4 + S$

Table 2
Electrochemical reactions and standard reduction potentials at 25°C

Reaction	E^o (V) at 25°C[a]
Stepwise anodic reactions	
R33. $Cu_2S = CuS + Cu^{2+} + 2e^-$	0.491
R34. $CuS = Cu^{2+} + S + 2e^-$	0.631
Cathodic reactions	
R35. $0.5O_2 + 2H^+ + 2e^- = H_2O$	1.230
Surface blockage by hydroxide	
R36. $Cu_2S + 2H_2O = Cu(OH)_2(ads) + 2H^+ + CuS + 2e^-$	0.680
R37. $CuS + 2H_2O = Cu(OH)_2\ (ads) + 2H^+ + 2e^-$	0.820
Surface activation by anions	
R38. $Cu_2S + X = (CuX)^{2+}(ads) + CuS + 2e^-$ ($X = H_2O, SO_4^{2-}, Cl^-, ClO_4^-, NO_3^-$)	
R39. $CuS + Cl^- = CuCl^+ + S + 2e^-$	0.619
Anodic reactions involving disulfide and chloride species	
R40. $2H_2S = 4H^+ + S_2^{2-} + 2e^-$	0.700
R41. $2CuS = 2Cu^{2+} + S_2^{2-} + 2e^-$	1.675
R42. $CuS + 2Cl^- = CuCl_2^- + S + 2e^-$	0.792
R43. $CuS_2 = Cu^{2+} + 2S + 2e^-$	0.715 (0.410 for NiS_2)[b]
R44. $2CuS + 3H_2O + Cl^- = Cu_2Cl(OH)_3 + 2S + 3H^+ + 4e^-$	0.742
R45. $CuS + Cl^- + H_2O = Cu(OH)Cl + S + H^+ + 2e^-$	0.622
R46. $2CuS = CuS_2 + Cu^{2+} + 2e^-$	0.525 (0 V for NiS_2)[b]
R47. $CuFeS_2 = CuS_2 + Fe^{2+} + 2e^-$	0.134
Mechanism for chloride assisted dissolution of CuS	
R48. $CuS + H^+ + Cl^- = Cu(SH)Cl$	
R49. $Cu(SH)Cl + H_2O = Cu(OH)Cl + S + 2H^+ + 2e^-$	
R50. $Cu(OH)Cl + HSO_4^- = Cu(SO_4)^0 + H_2O + Cl^-$	

a. data from HSC 6.1 data base or calculated in the present study (see text)
b. corresponding values for couples involving NiS, NiS_2, and Ni^{2+}.

Table 3
Equilibrium constants

Reaction		a Pb(II)	a Cu(II)	b Fe(II)	b Cu(II)
$M^{2+} + S_2O_3^{2-}$	$= M(S_2O_3)^0$	$10^{2.42}$	$10^{2.4}$	$10^{2.00}$	$10^{2.4}$
$M^{2+} + 2S_2O_3^{2-}$	$= M(S_2O_3)_2^{2-}$	$10^{4.86}$	$10^{5.4}$	-	-
$M^{2+} + CO_3^{2-}$	$= M(CO_3)^0$	10^{7}	$10^{6.77}$	$10^{5.69}$	$10^{6.5}$
$M^{2+} + 2CO_3^{2-}$	$= M(CO_3)_2^{2-}$	10^{9}	10^{10}	-	-
$M^{2+} + OH^-$	$= M(OH)^+$	$10^{6.9}$	$10^{6.27}$	$10^{4.67}$ ($10^{4.70}$)	$10^{5.98}$ ($10^{5.86}$)
$M^{2+} + 2OH^-$	$= M(OH)_2^0$	$10^{10.8}$	$10^{12.5}$	-	-
$M^{2+} + Cl^-$	$= M(Cl)^+$	$10^{1.6}$	$10^{0.6}$	-	-
$M^{2+} + 2Cl^-$	$= M(Cl)_2^0$	$10^{1.8}$	$10^{0.7}$	-	-
$M^{2+} + SO_4^{2-}$	$= M(SO_4)^0$	$10^{2.75}$	$10^{2.36}$	-	-
$M^{2+} + NO_3^-$	$= M(NO_3)^+$	$10^{1.2}$	$10^{0.5}$	-	-
$M^{2+} + 2NO_3^-$	$= M(NO_3)_2^0$	$10^{1.4}$	$10^{-0.4}$	-	-
$M^{2+} + 2OH^-$	$= M(OH)_2(s)$	$10^{19.9}$	$10^{19.8}$	$10^{15.0}$ ($10^{14.0}$)	$10^{21.6}$ ($10^{20.0}$)
$M^{2+} + C_2O_4^{2-}$	$= M(C_2O_4)(s)$	$10^{9.1}$	$10^{9.6}$	-	-
$M^{2+} + CO_3^{2-}$	$= M(CO_3)(s)$	10^{7}	$10^{6.77}$	$10^{8.27}$	$10^{9.85}$
$M^{2+} + H_2O$	$= MO(s) + 2H^+$	-	-	$10^{-14.5}$ ($10^{-11.1}$)	$10^{-7.71}$ ($10^{-5.70}$)
$M^{2+} + SO_4^{2-}$	$= M(SO_4)(s)$	-	-	$10^{-1.93}$ ($10^{0.70}$)	$10^{-3.0}$ ($10^{-0.38}$)
$M^{2+} + S^{2-}$	$= MS(s)$	-	-	$10^{16.9}$ ($10^{15.8}$)	$10^{36.4}$ ($10^{31.8}$)
$M^{2+} + 3HS^-$	$= M(HS)_3^-$	-	-	$10^{2.71c}$	$10^{6.23c}$
$M^{2+} + 2HS^-$	$= M(HS)_2^0$	-	-	$10^{2.2c}$	10^{8d}
$M^{2+} + S_2^{2-}$	$= MS_2(s)$	-	-	10^{26}	10^{39d}

a. At 25 ^oC, from Sillen and Martell (1964), Hogfeldt (1982).
b. At 25^oC, from HSC 6.1 database, values in parentheses are for 90^oC; inconsistency of values in columns a and b for Cu(II) from different references is due to differences in ionic strength and/or methods of measurements .
c. From Young et al. (2003)
d. Predicted values in this work based on Fig. 3a

Table 4
Test conditions used by Cheng and Lawson (1991a,b)

Test	T (^oC)	size (μm)	$[H_2SO_4]$ (mol dm^{-3})	NaCl (mol dm^{-3})	$[O_2]$ (%)	$[O_2]$ (mol m^{-3})	10^5 k_{ss} (s^{-1})
Data for covellite							
D1	90	13	0.5	0.5	5	0.039	1
D2					21	0.164	2
D3					59	0.461	3
D4					100	0.782	4
E1	90	13	0.5	0.1	100	0.741	0.7
E2				0.25			2
E3				0.5			3
E4				2.0			4
F1	90	13	0.005	0.5	100	0.716	2
F2			0.02				3
F3			0.50				4
F4			2.0				4
G1	85	58	0.5	0.5	100		0.9
G2		28					2
Data for chalcocite							
A1	85	23	0.5	0.5	5		2.5
A2					21		9.5
A3					39		18.7
A4					59		31.8
A5					81		30.7
A6					100		42.7
B1	85	31	0.5	0.02	100		3.7
B2				0.10			16.2
B3				0.25			32.3
B4				0.50			36.5
B5				2.0			39.0

1000 rpm, k_{ss} values are based on slopes of linear relationships as in Fig. 5 (see text)

Table 5
Calculated mass transfer coefficients of Y to particles suspended in water

Particle	size (μm)	D_Y (m^2 s^{-1})[a]	υ (m^2 s^{-1})[b]	Δρ/ρ	Gr	Sc	Sh	k_m (m s^{-1})[c]
CuS	28	6 x10^{-9}	2.5 x 10^{-7}	0.78	2.68	42	4.67	1x10^{-3}(at 85°C)

a. Based on Stokes-Einstein equation (Cussler, 1997) at 85°C
b. Haywood, 1990.
c. Eqs. 5-8